# Study of the $\psi_2(3823)$ and $\chi_{c1}(3872)$ states in $B^+ \to (J/\psi \pi^+ \pi^-) K^+$ decays

## The LHCb collaboration

*E-mail:* Ivan.Belyaev@itep.ru

ABSTRACT: The decays $B^+ \to J/\psi \pi^+ \pi^- K^+$ are studied using a data set corresponding to an integrated luminosity of $9\,\mathrm{fb}^{-1}$ collected with the LHCb detector in proton-proton collisions between 2011 and 2018. Precise measurements of the ratios of branching fractions with the intermediate $\psi_2(3823)$, $\chi_{c1}(3872)$ and $\psi(2S)$ states are reported. The values are

$$\frac{\mathcal{B}_{B^+\to\psi_2(3823)K^+} \times \mathcal{B}_{\psi_2(3823)\to J/\psi\pi^+\pi^-}}{\mathcal{B}_{B^+\to\chi_{c1}(3872)K^+} \times \mathcal{B}_{\chi_{c1}(3872)\to J/\psi\pi^+\pi^-}} = (3.56 \pm 0.67 \pm 0.11) \times 10^{-2},$$

$$\frac{\mathcal{B}_{B^+\to\psi_2(3823)K^+} \times \mathcal{B}_{\psi_2(3823)\to J/\psi\pi^+\pi^-}}{\mathcal{B}_{B^+\to\psi(2S)K^+} \times \mathcal{B}_{\psi(2S)\to J/\psi\pi^+\pi^-}} = (1.31 \pm 0.25 \pm 0.04) \times 10^{-3},$$

$$\frac{\mathcal{B}_{B^+\to\chi_{c1}(3872)K^+} \times \mathcal{B}_{\chi_{c1}(3872)\to J/\psi\pi^+\pi^-}}{\mathcal{B}_{B^+\to\psi(2S)K^+} \times \mathcal{B}_{\psi(2S)\to J/\psi\pi^+\pi^-}} = (3.69 \pm 0.07 \pm 0.06) \times 10^{-2},$$

where the first uncertainty is statistical and the second is systematic. The decay of $B^+ \to \psi_2(3823)K^+$ with $\psi_2(3823) \to J/\psi \pi^+ \pi^-$ is observed for the first time with a significance of 5.1 standard deviations. The mass differences between the $\psi_2(3823)$, $\chi_{c1}(3872)$ and $\psi(2S)$ states are measured to be

$$m_{\chi_{c1}(3872)} - m_{\psi_2(3823)} = 47.50 \pm 0.53 \pm 0.13\,\mathrm{MeV}/c^2,$$
$$m_{\psi_2(3823)} - m_{\psi(2S)} = 137.98 \pm 0.53 \pm 0.14\,\mathrm{MeV}/c^2,$$
$$m_{\chi_{c1}(3872)} - m_{\psi(2S)} = 185.49 \pm 0.06 \pm 0.03\,\mathrm{MeV}/c^2,$$

resulting in the most precise determination of the $\chi_{c1}(3872)$ mass. The width of the $\psi_2(3823)$ state is found to be below $5.2\,\text{MeV}$ at 90% confidence level. The Breit-Wigner width of the $\chi_{c1}(3872)$ state is measured to be

$$\Gamma^{\text{BW}}_{\chi_{c1}(3872)} = 0.96\,^{+\,0.19}_{-\,0.18} \pm 0.21\,\text{MeV}\,,$$

which is inconsistent with zero by 5.5 standard deviations.

# Contents

## 1 Introduction

The observation of a narrow $\chi_{c1}(3872)$ state in the $J/\psi\pi^+\pi^-$ mass spectrum of $B^+ \to J/\psi\pi^+\pi^-K^+$ decays by the Belle collaboration in 2003 [1] has led to a renewed interest in the study of hadrons containing heavy quarks. Many new charmonium-like states have since been observed [2]. Some of the new states are unambiguously interpreted as conventional $c\bar{c}$ states, some are manifestly exotic [3–9], while for the others a definite interpretation is still missing [10–12]. Despite the large amount of experimental data [13–40], the nature of the $\chi_{c1}(3872)$ state is still unclear. Several interpretations have been proposed, such as a conventional $\chi_{c1}(2P)$ state [41], a molecular state [42–44], a tetraquark [45], a $c\bar{c}g$ hybrid state [46], a vector glueball [47] or a mixed state [48, 49]. Precise measurements of the resonance parameters, namely the mass and the width, are crucial for the correct interpretation of the state. Comparison of the decays of beauty hadrons with final states involving the $\chi_{c1}(3872)$ particle and those involving other charmonium resonances can shed light on the production mechanism, in particular, on the role of $D^0\overline{D}^{*0}$ rescattering [50].

A recent analysis of $D^0\overline{D}^0$ and $D^+D^-$ mass spectra, performed by the LHCb collaboration [51], led to the observation of a new narrow state, $\psi_3(3842)$, interpreted as a spin-3 component of the D-wave charmonium triplet, $\psi_3(1^3D_3)$ state [52, 53], and a precise measurement of the mass of the vector component of this triplet, the $\psi(3770)$ state. Evidence for the third, tensor component of the triplet, the $\psi_2(3823)$ state,[1] was reported by the Belle collaboration in the $B \to (\psi_2(3823) \to \chi_{c1}\gamma)K$ decays [55]. This

---

[1]A hint for this state was reported in 1994 by the E705 experiment in studies of the $J/\psi\pi^+\pi^-$ final state in pion-lithium collisions with a statistical significance of 2.8 standard deviations [54].

was confirmed by the BES III collaboration with a significance in excess of 5 standard deviations [56]. The partial decay widths of the $\psi_2(3823)$ resonance are calculated to be $\Gamma_{\psi_2(3823)\to\chi_{c1}\gamma} = 215\,\mathrm{keV}$ [57], $\Gamma_{\psi_2(3823)\to\chi_{c2}\gamma} = 59\,\mathrm{keV}$ [57], $\Gamma_{\psi_2(3823)\to ggg} = 36\,\mathrm{keV}$ [58], and $\Gamma_{\psi_2(3823)\to J/\psi\pi\pi} \simeq 160\,\mathrm{keV}$ [59], corresponding to a total width of 470 keV and a branching fraction $\mathcal{B}_{\psi_2(3823)\to J/\psi\pi\pi}$ of 34% [60]. The predicted width is much smaller than the upper limit of 16 MeV at 90% confidence level (CL) set by the BES III collaboration [56].

In this paper, a sample of $B^+ \to (X_{c\bar{c}} \to J/\psi\,\pi^+\pi^-)\,K^+$ decays[2] is analysed, where $X_{c\bar{c}}$ denotes the $\psi_2(3823)$, $\chi_{c1}(3872)$ or $\psi(2S)$ state and the $J/\psi$ meson is reconstructed in the $\mu^+\mu^-$ final state. The study is based on proton-proton (pp) collision data, corresponding to an integrated luminosity of 1, 2, and $6\,\mathrm{fb}^{-1}$, collected with the LHCb detector at centre-of-mass energies of 7, 8, and 13 TeV, respectively. This data sample allows studies of the properties of the $\psi_2(3823)$ and $\chi_{c1}(3872)$ states produced in B decay recoiling against a kaon. The presence of the $\psi(2S)$ state in the same sample provides a convenient sample for normalisation and reduction of potential systematic uncertainties. A complementary measurement using inclusive $b \to (\chi_{c1}(3872) \to J/\psi\,\pi^+\pi^-)\,X$ decays and a data set, corresponding to an integrated luminosity of 1 and $2\,\mathrm{fb}^{-1}$, collected at the centre-of-mass energies of 7 and 8 TeV, is reported in ref. [61]. This gives a determination of the resonance parameters for the $\chi_{c1}(3872)$ state with an unprecedented precision, including searches for the poles of the complex Flatté-like amplitude.

## 2 Detector and simulation

The LHCb detector [62, 63] is a single-arm forward spectrometer covering the pseudorapidity range $2 < \eta < 5$, designed for the study of particles containing b or c quarks. The detector includes a high-precision tracking system consisting of a silicon-strip vertex detector surrounding the pp interaction region [64], a large-area silicon-strip detector located upstream of a dipole magnet with a bending power of about 4 Tm, and three stations of silicon-strip detectors and straw drift tubes [65, 66] placed downstream of the magnet. The tracking system provides a measurement of the momentum of charged particles with a relative uncertainty that varies from 0.5% at low momentum to 1.0% at $200\,\mathrm{GeV}/c$. The momentum scale is calibrated using samples of $J/\psi \to \mu^+\mu^-$ and $B^+ \to J/\psi\,K^+$ decays collected concurrently with the data sample used for this analysis [67, 68]. The relative accuracy of this procedure is estimated to be $3 \times 10^{-4}$ using samples of other fully reconstructed b hadrons, $\Upsilon$ and $K_S^0$ mesons. The minimum distance of a track to a primary pp-collision vertex (PV), the impact parameter (IP), is measured with a resolution of $(15 + 29/p_T)\,\mu\mathrm{m}$, where $p_T$ is the component of the momentum transverse to the beam, in $\mathrm{GeV}/c$. Different types of charged hadrons are distinguished using information from two ring-imaging Cherenkov detectors (RICH) [69]. Photons, electrons and hadrons are identified by a calorimeter system consisting of scintillating-pad and preshower detectors, an electromagnetic and a hadronic calorimeter. Muons are identified by a system composed of alternating layers of iron and multiwire proportional chambers [70].

---

[2]Inclusion of charge-conjugate states is implied throughout the paper.

The online event selection is performed by a trigger [71], which consists of a hardware stage, based on information from the calorimeter and muon systems, followed by a software stage, which applies a full event reconstruction. The hardware trigger selects muon candidates with high transverse momentum or dimuon candidates with a high value of the product of the $p_T$ of each muon. In the software trigger two oppositely charged muons are required to form a good-quality vertex that is significantly displaced from every PV, with a dimuon mass exceeding $2.7\,\mathrm{GeV}/c^2$.

Simulated events are used to describe the signal shapes and to compute efficiencies, needed to determine the branching fraction ratios. In the simulation, pp collisions are generated using PYTHIA [72] with a specific LHCb configuration [73]. Decays of unstable particles are described by the EVTGEN package [74], in which final-state radiation is generated using PHOTOS [75]. The $\psi_2(3823) \to \mathrm{J}/\psi\,\pi^+\pi^-$ decays are simulated using a phase-space model. The $\chi_{c1}(3872) \to \mathrm{J}/\psi\,\pi^+\pi^-$ decays are simulated proceeding via the S-wave $\mathrm{J}/\psi\,\rho^0$ intermediate state [34]. For the $\psi(2S)$ decays the model described in refs. [76–79] is used. The interaction of the generated particles with the detector, and its response, are implemented using the GEANT4 toolkit [80, 81] as described in ref. [82]. To account for imperfections in the simulation of charged-particle reconstruction, the track reconstruction efficiency determined from simulation is corrected using data-driven techniques [83].

## 3   Event selection

Candidate $\mathrm{B}^+ \to \mathrm{J}/\psi\,\pi^+\pi^-\mathrm{K}^+$ decays are reconstructed using the $\mathrm{J}/\psi \to \mu^+\mu^-$ decay mode. A loose preselection similar to refs. [37, 84–94] is applied, followed by a multivariate classifier based on a decision tree with gradient boosting (BDT) [95].

Muon, pion and kaon candidates are identified by combining information from the RICH, calorimeter and muon detectors [96]. The transverse momentum of muon (hadron) candiates is required to be larger than $550\,(220)\,\mathrm{MeV}/c$. To allow for efficient particle identification, kaons and pions are required to have a momentum between 3.2 and $150\,\mathrm{GeV}/c$. To reduce combinatorial background, only tracks that are inconsistent with originating from any reconstructed PV in the event are considered. Pairs of oppositely charged muons consistent with originating from a common vertex are combined to form $\mathrm{J}/\psi \to \mu^+\mu^-$ candidates. The reconstructed mass of the pair is required to be between 3.0 and $3.2\,\mathrm{GeV}/c^2$.

To form the $\mathrm{B}^+$ candidates, the selected $\mathrm{J}/\psi$ candidates are combined with a pair of oppositely charged pions and a positively charged kaon. Each $\mathrm{B}^+$ candidate is associated with the PV that yields the smallest $\chi^2_{\mathrm{IP}}$, where $\chi^2_{\mathrm{IP}}$ is defined as the difference in the vertex-fit $\chi^2$ of a given PV reconstructed with and without the particle under consideration. To improve the mass resolution for the $\mathrm{B}^+$ candidates, a kinematic fit [97] is performed. This fit constrains the mass of the $\mu^+\mu^-$ pair to the known mass of the $\mathrm{J}/\psi$ meson [2] and constraints the $\mathrm{B}^+$ candidate to originate from its associated PV. In addition, the measured decay time of the $\mathrm{B}^+$ candidate, calculated with respect to the associated PV, is required to be greater than $75\,\mu\mathrm{m}/c$. This requirement suppresses background from particles originating from the PV.
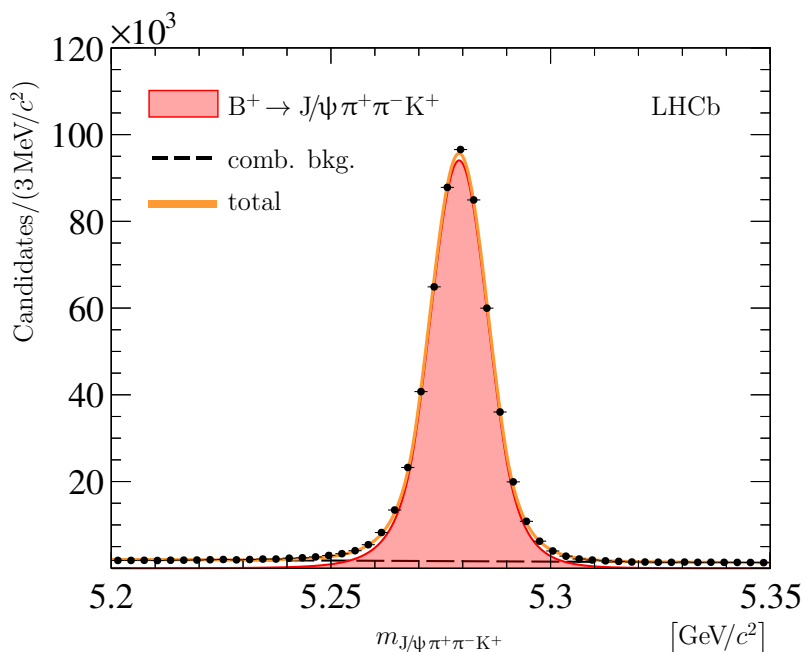
**Figure 1.** Distribution for the $J/\psi\pi^+\pi^-K^+$ mass for selected $B^+$ candidates (points with error bars). A fit, described in the text, is overlaid.

A BDT is used to further suppress the combinatorial background. It is trained using a simulated sample of $B^+ \to (\psi_2(3823) \to J/\psi\pi^+\pi^-)K^+$ decays as the signal. For the background, a sample of $J/\psi\pi^+\pi^+K^-$ combinations with same-sign pions in data, passing the preselection criteria and having the mass in the range between 5.20 and 5.35 GeV/$c^2$, is used. The $k$-fold cross-validation technique [98] with $k = 13$ is used to avoid introducing a bias in the BDT evaluation. The BDT is trained on variables related to the reconstruction quality, decay kinematics, decay time of $B^+$ candidate and the quality of the kinematic fit. The requirement on the BDT output is chosen to maximize $\varepsilon/(\alpha/2 + \sqrt{B})$ [99], where $\varepsilon$ is the signal efficiency for the $B^+ \to \psi_2(3823)K^+$ decays obtained from simulation; $\alpha = 5$ is the target signal significance in units of standard deviations; $B$ is the expected background yield within narrow mass windows centred at the known $B^+$ and $\psi_2(3823)$ masses [2]. The mass distribution of selected $B^+ \to J/\psi\pi^+\pi^-K^+$ candidates is shown in figure 1. The data are fit with a sum of a modified Gaussian function with power-law tails on both sides [100, 101] and a linear polynomial combinatorial background component. The $B^+$ signal yield is $(547.8 \pm 0.8) \times 10^3$ candidates.

## 4 Signal yields, masses and widths

The yields for the $B^+ \to (X_{c\bar{c}} \to J/\psi\pi^+\pi^-)K^+$ decays are determined using a two-dimensional unbinned extended maximum-likelihood fit to the $J/\psi\pi^+\pi^-K^+$ mass, $m_{J/\psi\pi^+\pi^-K^+}$, and the $J/\psi\pi^+\pi^-$ mass, $m_{J/\psi\pi^+\pi^-}$, distributions. The fit is performed simultaneously in the three non-overlapping regions

- $3.67 \le m_{J/\psi\pi^+\pi^-} < 3.70\,\text{GeV}/c^2$,

- $3.80 \leq m_{\text{J/}\psi\pi^+\pi^-} < 3.85\,\text{GeV}/c^2$,

- $3.85 \leq m_{\text{J/}\psi\pi^+\pi^-} < 3.90\,\text{GeV}/c^2$,

corresponding to the $B^+ \to \psi(2S)K^+$, $B^+ \to \psi_2(3823)K^+$ and $B^+ \to \chi_{c1}(3872)K^+$ decays. For each of the three regions the $\text{J/}\psi\pi^+\pi^-K^+$ mass is restricted to $5.20 \leq m_{\text{J/}\psi\pi^+\pi^-K^+} < 5.35\,\text{GeV}/c^2$. To improve the resolution on the $\text{J/}\psi\pi^+\pi^-$ mass and to eliminate a small correlation between $m_{\text{J/}\psi\pi^+\pi^-K^+}$ and $m_{\text{J/}\psi\pi^+\pi^-}$ variables, the $m_{\text{J/}\psi\pi^+\pi^-}$ variable is computed using a kinematic fit [97] that constrains the mass of the $B^+$ candidate to its known value [2]. In each region, the fit function is defined as a sum of four components:

1. signal $B^+ \to X_{c\bar{c}}K^+$ decays parameterised as a product of the $B^+$ and $X_{c\bar{c}}$ signal templates described in detail in the next paragraph;

2. contribution from the decays $B^+ \to (\text{J/}\psi\pi^+\pi^-)_{\text{NR}}\,K^+$ with no narrow intermediate $X_{c\bar{c}}$ state, parameterised as a product of the $B^+$ signal template and a linear function of $m_{\text{J/}\psi\pi^+\pi^-}$;

3. random combinations of $X_{c\bar{c}}$ and $K^+$ candidates, parameterised as a product of the $X_{c\bar{c}}$ signal template and a linear function of $m_{\text{J/}\psi\pi^+\pi^-K^+}$;

4. random $\text{J/}\psi\pi^+\pi^-K^+$ combinations, described below.

The templates for the $B^+$ signals are described by a modified Gaussian function with power-law tails on both sides of the distribution [100, 101]. The tail parameters are fixed to the values obtained from simulation. The narrow $X_{c\bar{c}}$ signal templates are parameterised with S-wave relativistic Breit-Wigner functions convolved with the mass resolution. Due to the proximity of the $\chi_{c1}(3872)$ state to the $D^0\overline{D}^{*0}$ threshold, modelling this component as a Breit-Wigner function may not be adequate [102–106]. However, the analysis from ref. [61] demonstrates that a good description of data is obtained with a Breit-Wigner lineshape when the mass resolution is included. The mass resolution is described by a symmetric modified Gaussian function with power-law tails on both sides of the distribution, with the parameters fixed to the values from simulation. In the template for the $B^+$ signal, the peak-position parameter is shared between all three decays and allowed to vary in the fit. The mass resolutions used in the $B^+$ and $X_{c\bar{c}}$ signal templates are fixed to the values determined from simulation, but are corrected by common scale factors, $f_{B^+}$ and $f_{X_{c\bar{c}}}$, to account for a small discrepancy in the mass resolution between data and simulation. The masses of the $X_{c\bar{c}}$ signal templates, as well as the Breit-Wigner widths for the $\psi_2(3823)$ and $\chi_{c1}(3872)$ states, are free fit parameters, while the width in the template for the $\psi(2S)$ signal is fixed to its known value [2]. The combinatorial-background component is modelled with a smooth two-dimensional function

$$\mathcal{E}(m_{\text{J/}\psi\pi^+\pi^-K^+}) \times \mathcal{P}_{3,4}(m_{\text{J/}\psi\pi^+\pi^-}) \times P_{2D}(m_{\text{J/}\psi\pi^+\pi^-K^+}, m_{\text{J/}\psi\pi^+\pi^-}), \tag{4.1}$$

where $\mathcal{E}(m_{\text{J/}\psi\pi^+\pi^-K^+})$ is an exponential function, $\mathcal{P}_{3,4}(m_{\text{J/}\psi\pi^+\pi^-})$ is a three-body phase-space function [107], and $P_{2D}$ is a two-dimensional positive bilinear function, which accounts

| Parameter | $B^+ \to \psi(2S)K^+$ | $B^+ \to \psi_2(3823)K^+$ | $B^+ \to \chi_{c1}(3872)K^+$ |
|---|---|---|---|
| $N_{B^+ \to X_{c\bar{c}}K^+}$ | $(81.14 \pm 0.29) \times 10^3$ | $137 \pm 26$ | $4230 \pm 70$ |
| $\delta m_{X_{c\bar{c}}}$ $[\mathrm{MeV}/c^2]$ | — | $137.98 \pm 0.53$ | $185.49 \pm 0.06$ |
| $\Gamma_{X_{c\bar{c}}}$ $[\mathrm{MeV}]$ | $0.29\,(\mathrm{fixed})$ | $0\,{}^{+\,0.68}_{-\,0.00}$ | $0.96\,{}^{+\,0.19}_{-\,0.18}$ |
| $f_{B^+}$ | $1.052 \pm 0.003$ | | |
| $f_{X_{c\bar{c}}}$ | $1.048 \pm 0.004$ | | |

**Table 1**. Parameters of interest and derived quantities from the simultaneous unbinned extended maximum-likelihood two-dimensional fit. Results and statistical uncertainties are shown for the three fit regions.

for small non-factorizable effects. For the considered fit ranges $\mathcal{P}_{3,4}(m_{J/\psi\,\pi^+\pi^-})$ is close to a constant.

The $J/\psi\,\pi^+\pi^-K^+$ and $J/\psi\,\pi^+\pi^-$ mass distributions together with projections of the simultaneous unbinned maximum-likelihood fit are shown in figure 2. Signal yields $N_{B^+ \to X_{c\bar{c}}K^+}$, calculated mass differences $\delta m_{X_{c\bar{c}}} \equiv m_{X_{c\bar{c}}} - m_{\psi(2S)}$, Breit-Wigner widths $\Gamma_{X_{c\bar{c}}}$ and resolution scale factors are listed in table 1. The fit model is tested using pseudoexperiments and no bias is found in the results and their associated uncertainties. The masses of $B^+$ and $\psi(2S)$ mesons are found to be compatible with their known values [2]. The fit component corresponding to the $B^+ \to (J/\psi\,\pi^+\pi^-)_{\mathrm{NR}}\,K^+$ is found to be negligible for the $\psi(2S)$ region, dominant for the $\psi_2(3823)$ region and small for the $\chi_{c1}(3872)$ region. The fit component corresponding to the random $X_{c\bar{c}}K^+$ combinations is negligible for all fit regions. The statistical significance of the observed $B^+ \to (\psi_2(3823) \to J/\psi\,\pi^+\pi^-)\,K^+$ signal over the background-only hypothesis is estimated to be 5.1 standard deviations using Wilks' theorem [108]. The significance is confirmed by simulating a large number of pseudoexperiments according to the background distribution observed in data.

The likelihood profiles for the Breit-Wigner widths of $\psi_2(3823)$ and $\chi_{c1}(3872)$ states are presented in figure 3. From these profiles the Breit-Wigner width of the $\chi_{c1}(3872)$ state is found to be inconsistent with zero by 5.5 standard deviations, while for the $\psi_2(3823)$ state the width is consistent with zero.

## 5 Ratios of branching fractions

Ratios of branching fractions, $\mathcal{R}_Y^X$, are defined as

$$\mathcal{R}_Y^X \equiv \frac{\mathcal{B}_{B^+ \to XK^+} \times \mathcal{B}_{X \to J/\psi\,\pi^+\pi^-}}{\mathcal{B}_{B^+ \to YK^+} \times \mathcal{B}_{Y \to J/\psi\,\pi^+\pi^-}}\,, \tag{5.1}$$

where X, Y stand for either the $\psi_2(3823)$, $\chi_{c1}(3872)$ or $\psi(2S)$ states. They are estimated as

$$\mathcal{R}_Y^X = \frac{N_{B^+ \to XK^+}}{N_{B^+ \to YK^+}} \times \frac{\varepsilon_{B^+ \to YK^+}}{\varepsilon_{B^+ \to XK^+}}\,, \tag{5.2}$$

where $N$ is the signal yield reported in table 1 and $\varepsilon$ denotes the efficiency of the corresponding decay. The efficiency is defined as the product of geometric acceptance, re-
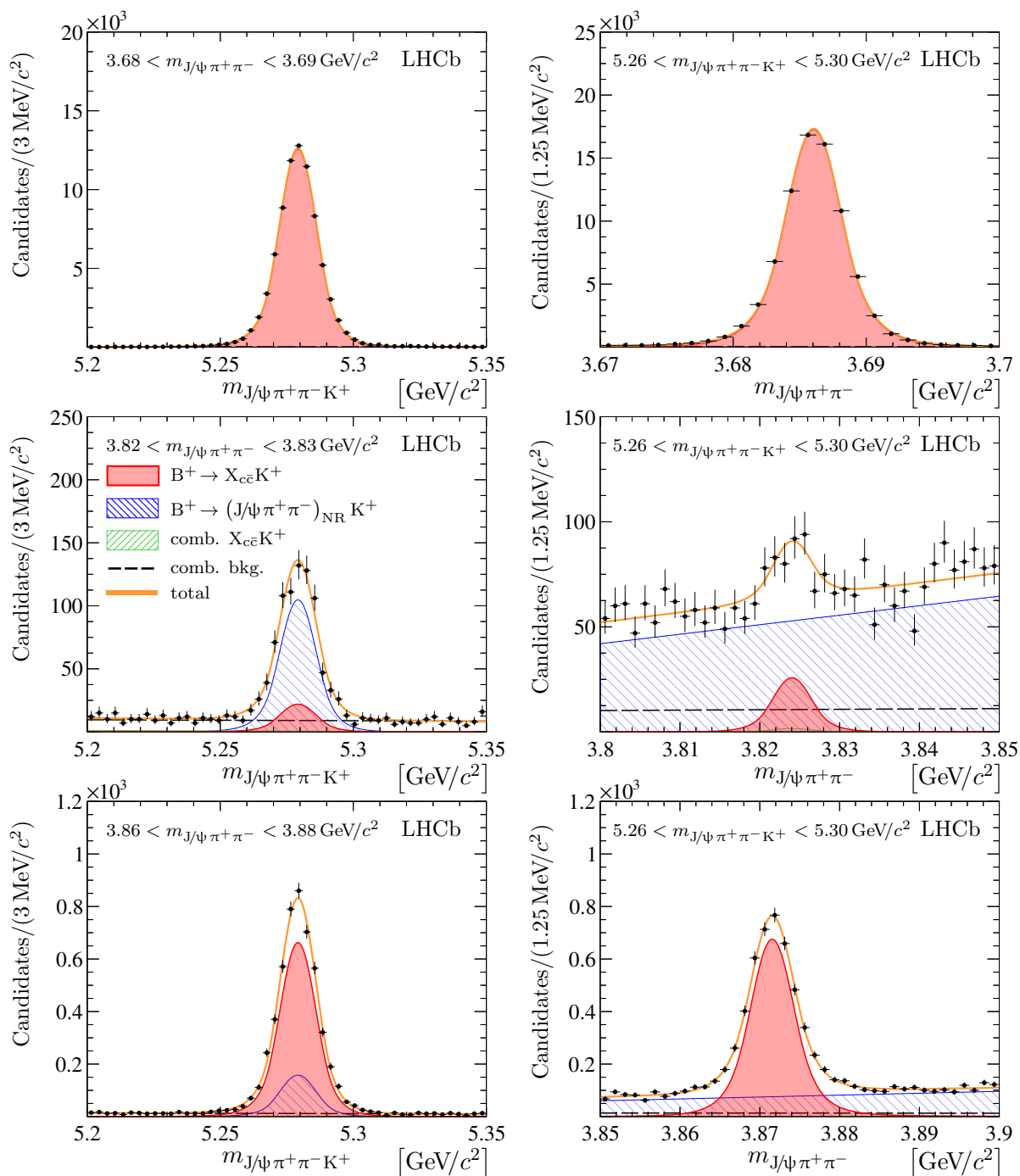
**Figure 2**. Distributions of the (left) $J/\psi \pi^+\pi^- K^+$ and (right) $J/\psi \pi^+\pi^-$ mass for selected (top) $B^+ \to \psi(2S)K^+$, (middle) $B^+ \to \psi_2(3823)K^+$ and (bottom) $B^+ \to \chi_{c1}(3872)K^+$ candidates shown as points with error bars. A fit, described in the text, is overlaid.
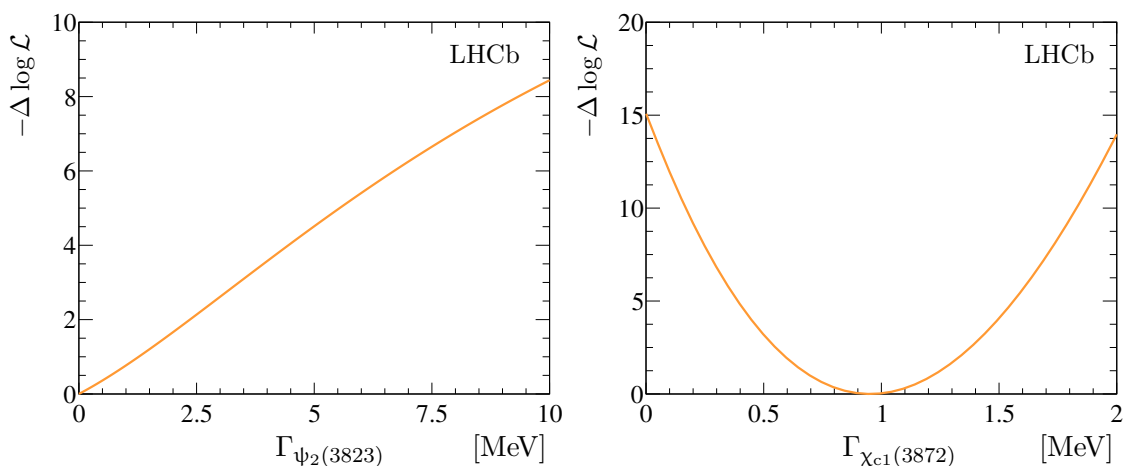
**Figure 3**. Likelihood profiles for the Breit-Wigner width of (left) $\psi_2(3823)$ and (right) $\chi_{c1}(3872)$ states.

construction, selection, hadron identification and trigger efficiencies, where each subsequent efficiency is defined with respect to the previous one. All of the contributions, except that of the hadron-identification efficiency, are determined using simulated samples. The hadron-identification efficiency is determined using large calibration samples of $D^{*+} \to \left( D^0 \to K^- \pi^+ \right) \pi^+$, $K_S^0 \to \pi^+ \pi^-$ and $D_s^+ \to (\phi \to K^+ K^-) \pi^+$ decays selected in data for kaons and pions [69, 109]. The ratios of the efficiencies are determined to be

$$\frac{\varepsilon_{B^+ \to \chi_{c1}(3872)K^+}}{\varepsilon_{B^+ \to \psi_2(3823)K^+}} = 1.098 \pm 0.003 \,,$$

$$\frac{\varepsilon_{B^+ \to \psi(2S)K^+}}{\varepsilon_{B^+ \to \psi_2(3823)K^+}} = 0.778 \pm 0.003 \,, \tag{5.3}$$

$$\frac{\varepsilon_{B^+ \to \psi(2S)K^+}}{\varepsilon_{B^+ \to \chi_{c1}(3872)K^+}} = 0.708 \pm 0.003 \,,$$

where the uncertainty reflects the limited size of the simulated samples. Other sources of systematic uncertainty are discussed in the following section. The ratios of the efficiencies differ from unity mostly due to the different pion momentum spectra in the different $X_{c\bar{c}} \to J/\psi \, \pi^+ \pi^-$ decays.

## 6    Systematic uncertainty

Due to the similar decay topologies, systematic uncertainties largely cancel in the ratios $\mathcal{R}_Y^X$. The remaining contributions are listed in table 2 and are discussed below.

The systematic uncertainty related to the signal and background shapes is investigated using alternative parameterisations. A generalized Student's $t$-distribution [110], an Apollonios function [111] and a modified Novosibirsk function [112] are used as alternative models for the $B^+$ signal template. For the $X_{c\bar{c}}$ signal template, alternative parameterisations of the mass resolution, namely a symmetric variant of an Apollonios function [111], a Student's $t$-distribution and a sum of two Gaussian functions sharing the same mean are

| Source | $\mathcal{R}^{\psi_2(3823)}_{\chi_{c1}(3872)}$ | $\mathcal{R}^{\psi_2(3823)}_{\psi(2S)}$ | $\mathcal{R}^{\chi_{c1}(3872)}_{\psi(2S)}$ |
|---|---|---|---|
| Signal and background shapes | | | |
| $\quad$ $B^+$ signal template | 0.6 | 0.5 | 0.1 |
| $\quad$ $X_{c\bar{c}}$ signal template | 0.3 | 0.2 | 0.2 |
| $\quad$ Polynomial components | 2.5 | 2.7 | 0.2 |
| $\psi_2(3823)$ decay model | 0.2 | 0.2 | — |
| Efficiency corrections | < 0.1 | 0.2 | 0.2 |
| Trigger efficiency | 1.1 | 1.1 | 1.1 |
| Data-simulation agreement | 1.0 | 1.0 | 1.0 |
| Simulation sample size | 0.3 | 0.4 | 0.4 |
| Sum in quadrature | 3.0 | 3.2 | 1.6 |

**Table 2**. Relative systematic uncertainties (in %) for the ratios of branching fractions $\mathcal{R}^{X}_{Y}$.

considered. In addition, P-wave and D-wave relativistic Breit-Wigner functions are used as alternative $\psi_2(3823)$ signal templates, and the Blatt–Weisskopf barrier factors [113] are varied between 1.5 and $5\,\mathrm{GeV}^{-1}$. The width of the $\psi(2S)$ state, fixed in the fit, is varied between 270 and $302\,\mathrm{keV}$ [2]. The maximal deviations in the ratios $\mathcal{R}^{X}_{Y}$ with respect to the baseline fit model are taken as systematic uncertainties for each of the systematic signal model sources. For the systematic uncertainty related to the modelling of the smooth polynomial functions, pseudoexperiments with about $10^7$ simulated events (approximately 100 times large than data sample are generated with the baseline fit model and fitted with alternative background models. In this study the degree of the polynomial functions is varied from the first to the second order, separately for each fit component and each channel. In each case the ratio $\mathcal{R}^{X}_{Y}$ is computed and the maximal difference with respect to the baseline fit model is taken as a corresponding systematic uncertainty.

Since the decay model for $\psi_2(3823) \to J/\psi\,\pi^+\pi^-$ is unknown, a phase-space model is used in simulation. To probe the associated systematic uncertainty the model discussed in ref. [59] is used. This model accounts for the quantum-chromodynamics multipole expansion [114], as well as the effective description of the coupled-channel effects via hadronic-loop mechanism [115] with the interference phase $\Phi$ as a free parameter. The $\pi^+\pi^-$ mass spectrum and the angular distributions in the decay strongly depend on the phase $\Phi$, however, the efficiency for the $B^+ \to (\psi_2(3823) \to J/\psi\,\pi^+\pi^-)\,K^+$ decays is found to be stable. It varies within 0.2% with respect to the efficiency computed for the phase-space model when the unknown phase $\Phi$ varies in the range $-\pi \leq \Phi < \pi$.

An additional uncertainty arises from differences between the data and simulation, in particular differences in the reconstruction efficiency of charged-particle tracks. The track-finding efficiencies obtained from the simulation samples are corrected using data-

| Source | $m_{\psi_2(3823)} - m_{\psi(2S)}$ | $m_{\chi_{c1}(3872)} - m_{\psi(2S)}$ | $m_{\chi_{c1}(3872)} - m_{\psi_2(3823)}$ |
|---|---|---|---|
| Signal and background shapes | | | |
| $\quad$ B$^+$ signal template | 0.023 | 0.002 | 0.023 |
| $\quad$ X$_{c\bar{c}}$ signal template | 0.115 | 0.005 | 0.110 |
| $\quad$ Polynomial components | 0.070 | 0.001 | 0.070 |
| Momentum scale | 0.004 | 0.009 | 0.005 |
| B$^+$ mass uncertainty | 0.021 | 0.029 | 0.008 |
| Sum in quadrature | 0.138 | 0.031 | 0.133 |

**Table 3**. Systematic uncertainties (in MeV/$c^2$) for the mass splitting between the $\psi_2(3823)$, $\chi_{c1}(3872)$ and $\psi(2S)$ states.

driven techniques [83]. The uncertainties related to the correction factors, together with the uncertainty in the hadron-identification efficiency due to the finite size of the calibration samples [69, 109], are propagated to the ratio of total efficiencies using pseudoexperiments.

The systematic uncertainty related to the trigger efficiency is estimated using large samples of the B$^+ \to$ J/$\psi$K$^+$ and B$^+ \to \psi$(2S)K$^+$ decays by comparing the ratios of trigger efficiencies in data and simulation [84]. The imperfect data description by the simulation due to remaining effects is studied by varying the BDT selection criteria in ranges that lead to $\pm 20\%$ change in the measured efficiency. The resulting variations in the efficiency ratios do not exceed 1%, which is taken as a corresponding systematic uncertainty. The last systematic uncertainty considered for the ratio $\mathcal{R}_Y^X$ is due to the finite size of the simulated samples.

For each choice of the fit model, the statistical significance of the observed B$^+ \to (\psi_2(3823) \to$ J/$\psi \pi^+ \pi^-)$K$^+$ signal is calculated from fit to data using Wilks' theorem. The smallest significance found is 5.1 standard deviations, numerically close to the value obtained from the baseline fit model.

The systematic uncertainties on the mass differences between the $\psi_2(3823)$, $\chi_{c1}(3872)$ and $\psi$(2S) states are summarized in table 3. An important source of systematic uncertainty is due to the signal and background shapes. Different parameterisations of the signal templates and non-signal components, described above, are used as the alternative fit models. The maximal deviation in the mass differences with respect to the baseline results is assigned as the corresponding systematic uncertainty. The uncertainty in the momentum-scale calibration, important for mass measurements, e.g. refs. [51, 67, 68, 85, 90, 93, 94, 116–125], largely cancels for the mass differences. The associated systematic uncertainty is evaluated by varying the momentum scale within its known uncertainty [68] and repeating the fit. The J/$\psi \pi^+ \pi^-$ mass is computed constraining the mass of the B$^+$ candidate to the known value, $m_{\mathrm{B}^+} = 5279.25 \pm 0.26$ MeV/$c^2$ [2]. The uncertainty on the B$^+$ meson mass is propagated to the measured mass differences.

The main source of systematic uncertainty for the Breit-Wigner widths $\Gamma_{\psi_2(3823)}$ and $\Gamma_{\chi_{c1}(3872)}$ is due to the signal and background shapes. The maximal $\Gamma_{\chi_{c1}(3872)}$ deviation of $0.21\,\mathrm{MeV}$ is taken as the systematic uncertainty. For all the fits, the $\Gamma_{\psi_2(3823)}$ parameter is found to be consistent with zero, and an upper limit is obtained from analysis of the likelihood profile curve. The maximal value of the upper limits is conservatively taken as the estimate that accounts for the systematic uncertainty

$$\Gamma_{\psi_2(3823)} < 5.2\,(6.6)\,\mathrm{MeV} \text{ at } 90\,(95)\%\,\mathrm{CL}. \tag{6.1}$$

The systematic uncertainty due to the mismodelling of the experimental resolution in simulation is accounted for with the resolution scale factors $f_{\mathrm{B}+}$ and $f_{\mathrm{X}_{c\bar{c}}}$ and therefore is included as a part of the statistical uncertainty. A small dependency of the scale factor $f_{\mathrm{X}_{c\bar{c}}}$ on the dipion momentum for the $\psi(2S) \to \mathrm{J}/\psi\,\pi^+\pi^-$ decay is reported in ref. [61]. Such effect causes a bias in the effective scale factor for different decays due to slightly different dipion spectra. Such bias is found to be negligible with respect to the statistical uncertainty for the factor $f_{\mathrm{X}_{c\bar{c}}}$.

The analysis is carried out by neglecting any interference effects between the $\mathrm{X}_{c\bar{c}}$ resonances and other components. Such an assumption can bias the measurement of the mass and width-parameters associated to the $\mathrm{X}_{c\bar{c}}$ states. To account for such interference effects a full amplitude analysis is required, which is beyond the scope of this study. However, to estimate the possible effect of this assumption on the $\chi_{c1}(3872)$ mass and width-parameters, the background-subtracted $\mathrm{J}/\psi\,\pi^+\pi^-$ mass distribution in the $\chi_{c1}(3872)$ region is studied with the *sPlot* technique used for background subtraction [126] using the $\mathrm{J}/\psi\,\pi^+\pi^-\mathrm{K}^+$ mass as the discriminative variable. The distribution is fit with a model that accounts for the signal, coherent and incoherent backgrounds

$$\mathcal{F}(m) = \mathcal{N}\left(\left|\mathcal{A}_{\mathrm{BW}}(m) + b_{\mathrm{c}}(m)\,\mathrm{e}^{i\delta(m)}\right|^2 \circledast \mathfrak{R}\right) + b_{\mathrm{i}}^2(m), \tag{6.2}$$

where $\mathcal{A}_{\mathrm{BW}}(m)$ is a Breit-Wigner amplitude, convolved with the mass resolution function $\mathfrak{R}$, and $\mathcal{N}$ stands for a normalisation constant. The coherent and incoherent background components $b_{\mathrm{c}}(m)$ and $b_{\mathrm{i}}^2(m)$ are parameterised with polynomial functions. The relative interference phase $\delta(m)$ is taken to be constant for the narrow $3.85 \leq m_{\mathrm{J}/\psi\,\pi^+\pi^-} < 3.90\,\mathrm{GeV}/c^2$ region, $\delta(m) \equiv \delta_0$. An equally good description of data is achieved for totally incoherent ($b_{\mathrm{c}}(m) \equiv 0$) and coherent ($b_{\mathrm{i}}^2(m) \equiv 0$) background hypotheses, as well as for any intermediate scenarios with the phase $\delta_0$ close to $\frac{\pi}{2}$. The latter reflects a high symmetry of the observed $\chi_{c1}(3872)$ lineshape. For all scenarios, variations of the mass and width parameters are limited to $50\,\mathrm{keV}/c^2$ and $150\,\mathrm{keV}$, respectively.

## 7 Results and summary

The decay of $B^+ \to (\psi_2(3823) \to J/\psi\,\pi^+\pi^-)\,K^+$ is observed for the first time with a significance of 5.1 standard deviations. The signal yield of $137 \pm 26$ candidates, together with $4230 \pm 70$ $B^+ \to (\chi_{c1}(3872) \to J/\psi\,\pi^+\pi^-)\,K^+$ and $(81.14 \pm 0.29) \times 10^3$ $B^+ \to (\psi(2S) \to J/\psi\,\pi^+\pi^-)\,K^+$ signal candidates, allows for a precise determination of the ratios of the branching fractions

$$
\mathcal{R}_{\chi_{c1}(3872)}^{\psi_2(3823)} = \frac{\mathcal{B}_{B^+\to\psi_2(3823)K^+} \times \mathcal{B}_{\psi_2(3823)\to J/\psi\,\pi^+\pi^-}}{\mathcal{B}_{B^+\to\chi_{c1}(3872)K^+} \times \mathcal{B}_{\chi_{c1}(3872)\to J/\psi\,\pi^+\pi^-}} = (3.56 \pm 0.67 \pm 0.11) \times 10^{-2}\,,
$$

$$
\mathcal{R}_{\psi(2S)}^{\psi_2(3823)} = \frac{\mathcal{B}_{B^+\to\psi_2(3823)K^+} \times \mathcal{B}_{\psi_2(3823)\to J/\psi\,\pi^+\pi^-}}{\mathcal{B}_{B^+\to\psi(2S)K^+} \times \mathcal{B}_{\psi(2S)\to J/\psi\,\pi^+\pi^-}} = (1.31 \pm 0.25 \pm 0.04) \times 10^{-3}\,,
$$

$$
\mathcal{R}_{\psi(2S)}^{\chi_{c1}(3872)} = \frac{\mathcal{B}_{B^+\to\chi_{c1}(3872)K^+} \times \mathcal{B}_{\chi_{c1}(3872)\to J/\psi\,\pi^+\pi^-}}{\mathcal{B}_{B^+\to\psi(2S)K^+} \times \mathcal{B}_{\psi(2S)\to J/\psi\,\pi^+\pi^-}} = (3.69 \pm 0.07 \pm 0.06) \times 10^{-2}\,,
$$

where the first uncertainty is statistical and the second is systematic. The last ratio is in good agreement with, but significantly more precise than the value of $(4.0 \pm 0.4) \times 10^{-2}$, derived from ref. [2]. Only two ratios $\mathcal{R}_Y^X$ are statistically independent. The non-zero correlation coefficients are $+97\%$ for $\mathcal{R}_{\chi_{c1}(3872)}^{\psi_2(3823)}$ and $\mathcal{R}_{\psi(2S)}^{\psi_2(3823)}$, and $-7\%$ for $\mathcal{R}_{\chi_{c1}(3872)}^{\psi_2(3823)}$ and $\mathcal{R}_{\psi(2S)}^{\chi_{c1}(3872)}$. The product of branching fractions for the decay via the intermediate $\psi_2(3823)$ state is calculated to be

$$
\mathcal{B}_{B^+\to\psi_2(3823)K^+} \times \mathcal{B}_{\psi_2(3823)\to J/\psi\,\pi^+\pi^-} = (2.82 \pm 0.54 \pm 0.09 \pm 0.10) \times 10^{-7}\,,
$$

where the last uncertainty is due to the knowledge of the branching fractions for $B^+ \to \psi(2S)K^+$ and $\psi(2S) \to J/\psi\,\pi^+\pi^-$ decays [2]. Combined with the calculated value of $\mathcal{B}_{\psi_2(3823)\to J/\psi\,\pi\pi}$ [60] this yields $\mathcal{B}_{B^+\to\psi_2(3823)K^+} = (1.24 \pm 0.25) \times 10^{-6}$. This is smaller but more precise than the value of $(2.1 \pm 0.7) \times 10^{-5}$ derived from the measurement of $\mathcal{B}_{B^+\to\psi_2(3823)K^+} \times \mathcal{B}_{\psi_2(3823)\to\chi_{c1}\gamma} = (9.7 \pm 2.8 \pm 1.1) \times 10^{-6}$ by the Belle collaboration [55] and the estimate for $\mathcal{B}_{\psi_2(3823)\to\chi_{c1}\gamma}$ [60]. Within a factorization approach the branching fraction for the decay $B^+ \to \psi_2(3823)K^+$ vanishes, and a large value for this branching fraction requires a large contribution of the $D_s^{(*)+}\overline{D}^{(*)0}$ rescattering amplitudes in the $B^+ \to c\bar{c}K^+$ decays [60]. This measurement of the branching fraction for the $B^+ \to \psi_2(3823)K^+$ decay allows for a more precise estimation of the role of the $D_s^{(*)+}\overline{D}^{(*)0}$ rescattering mechanism [60].

Using a Breit−Wigner parameterisation, the mass differences between the $\psi_2(3823)$, $\chi_{c1}(3872)$ and $\psi(2S)$ states are found to be

$$
\begin{aligned}
m_{\chi_{c1}(3872)} - m_{\psi_2(3823)} &= \phantom{0}47.50 \pm 0.53 \pm 0.13 \,\mathrm{MeV}/c^2\,,\\
m_{\psi_2(3823)} - m_{\psi(2S)} &= 137.98 \pm 0.53 \pm 0.14 \,\mathrm{MeV}/c^2\,,\\
m_{\chi_{c1}(3872)} - m_{\psi(2S)} &= 185.49 \pm 0.06 \pm 0.03 \,\mathrm{MeV}/c^2\,.
\end{aligned}
$$

Only two from three mass differences are independent. Two non-zero correlation coefficients are $-93\%$ for $m_{\chi_{c1}(3872)} - m_{\psi_2(3823)}$ and $m_{\psi_2(3823)} - m_{\psi(2S)}$ and $+10\%$ for $m_{\chi_{c1}(3872)} - m_{\psi_2(3823)}$ and $m_{\chi_{c1}(3872)} - m_{\psi(2S)}$.

The Breit-Wigner width of the $\chi_{c1}(3872)$ state is found to be

$$\Gamma_{\chi_{c1}(3872)} = 0.96\,^{+\,0.19}_{-\,0.18} \pm 0.21\,\mathrm{MeV}\,,$$

which is inconsistent with zero by 5.5 standard deviations. The width of the $\psi_2(3823)$ state is found to be consistent with zero and an upper limit at $90\%\,(95\%)$ confidence level is set at

$$\Gamma_{\psi_2(3823)} < 5.2\,(6.6)\,\mathrm{MeV}\,.$$

The value of the Breit-Wigner width $\Gamma_{\chi_{c1}(3872)}$ agrees well with the value from the analysis of a large sample of $\chi_{c1}(3872) \to \mathrm{J}/\psi\,\pi^+\pi^-$ decays from the inclusive decays of beauty hadrons [61]. Using the known value of the $\psi(2S)$ mass [2], the Breit$-$Wigner masses for the $\psi_2(3823)$ and $\chi_{c1}(3872)$ states are computed to be

$$m_{\psi_2(3823)} = 3824.08 \pm 0.53 \pm 0.14 \pm 0.01\,\mathrm{MeV}/c^2\,,$$
$$m_{\chi_{c1}(3872)} = 3871.59 \pm 0.06 \pm 0.03 \pm 0.01\,\mathrm{MeV}/c^2\,,$$

where the last uncertainty is due to the knowledge of the $\psi(2S)$ mass. These are the most precise measurements of these masses.

The mass difference between $\chi_{c1}(3872)$ and $\psi(2S)$ states is more precise than the average reported in ref. [2]. It also agrees well with the measurement from ref. [61]. Taking into account a partial overlap of the data sets and correlated part of systematic uncertainty, the LHCb average mass difference and the mass of the $\chi_{c1}(3872)$ state are

$$m_{\chi_{c1}(3872)} - m_{\psi(2S)}\big|_{\mathrm{LHCb}} = 185.54 \pm 0.06\,\mathrm{MeV}/c^2\,,$$
$$m_{\chi_{c1}(3872)}\big|_{\mathrm{LHCb}} = 3871.64 \pm 0.06 \pm 0.01\,\mathrm{MeV}/c^2\,,$$

where the second uncertainty is due to the knowledge of the $\psi(2S)$ mass. The difference between the $m_{\chi_{c1}(3872)}$ mass, determined from the Breit-Wigner fit, and the $\mathrm{D}^0\mathrm{D}^{*0}$ threshold $\delta E \equiv (\,\mathrm{m}_{\mathrm{D}^0} + m_{\mathrm{D}^{*0}})\,c^2 - m_{\chi_{c1}(3872)}c^2$ is computed to be

$$\delta E = 0.12 \pm 0.13\,\mathrm{MeV}\,,$$
$$\delta E|_{\mathrm{LHCb}} = 0.07 \pm 0.12\,\mathrm{MeV}\,,$$

where the first value corresponds to the measurement performed in this analysis, while the second one is an average with results from ref. [61]. A value of $3871.70 \pm 0.11\,\mathrm{MeV}/c^2$ is taken for the threshold $\mathrm{m}_{\mathrm{D}^0} + m_{\mathrm{D}^{*0}}$, calculated from refs. [2, 61], accounting for the correlation due to the knowledge of the charged and neutral kaon masses between the measurements. The uncertainty on $\delta E$ is now dominated by the knowledge of kaon masses. These are the most precise measurements of the $\chi_{c1}(3872)$ mass and $\delta E$ parameter.

## Acknowledgments

## References

[1] Belle collaboration, *Observation of a narrow charmoniumlike state in exclusive* $B^\pm \rightarrow K^\pm\pi^+\pi^- J/\psi$ *decays*, *Phys. Rev. Lett.* **91** (2003) 262001 [hep-ex/0309032] [INSPIRE].

[2] Particle Data Group collaboration, *Review of particle physics*, *Phys. Rev. D* **98** (2018) 030001 [INSPIRE].

[3] Belle collaboration, *Observation of a resonancelike structure in the* $\pi^{+-}\psi'$ *mass distribution in exclusive* $B \rightarrow K\pi^{+-}\psi'$ *decays*, *Phys. Rev. Lett.* **100** (2008) 142001 [arXiv:0708.1790] [INSPIRE].

[4] Belle collaboration, *Observation of two resonance-like structures in the* $\pi^+\chi_{c1}$ *mass distribution in exclusive* $\bar{B}^0 \rightarrow K^-\pi^+\chi_{c1}$ *decays*, *Phys. Rev. D* **78** (2008) 072004 [arXiv:0806.4098] [INSPIRE].

[5] Belle collaboration, *Dalitz analysis of* $B \rightarrow K\pi^+\psi'$ *decays and the* $Z(4430)^+$, *Phys. Rev. D* **80** (2009) 031104 [arXiv:0905.2869] [INSPIRE].

[6] Belle collaboration, *Experimental constraints on the spin and parity of the* $Z(4430)^+$, *Phys. Rev. D* **88** (2013) 074026 [arXiv:1306.4894] [INSPIRE].

[7] LHCb collaboration, *Observation of the resonant character of the Z(4430)⁻ state*, *Phys. Rev. Lett.* **112** (2014) 222002 [arXiv:1404.1903] [INSPIRE].

[8] LHCb collaboration, *Model-independent confirmation of the Z(4430)⁻ state*, *Phys. Rev. D* **92** (2015) 112009 [arXiv:1510.01951] [INSPIRE].

[9] LHCb collaboration, *Evidence for an $\eta_c(1S)\pi^-$ resonance in $B^0 \to \eta_c(1S)K^+\pi^-$ decays*, *Eur. Phys. J. C* **78** (2018) 1019 [arXiv:1809.07416] [INSPIRE].

[10] S.L. Olsen, T. Skwarnicki and D. Zieminska, *Nonstandard heavy mesons and baryons: experimental evidence*, *Rev. Mod. Phys.* **90** (2018) 015003 [arXiv:1708.04012] [INSPIRE].

[11] N. Brambilla et al., *The $XYZ$ states: experimental and theoretical status and perspectives*, *Phys. Rept.* **873** (2020) 1 [arXiv:1907.07583] [INSPIRE].

[12] Y.-R. Liu, H.-X. Chen, W. Chen, X. Liu and S.-L. Zhu, *Pentaquark and tetraquark states*, *Prog. Part. Nucl. Phys.* **107** (2019) 237 [arXiv:1903.11976] [INSPIRE].

[13] CDF collaboration, *Observation of the narrow state $X(3872) \to J/\psi\pi^+\pi^-$ in $\bar{p}p$ collisions at $\sqrt{s} = 1.96\,TeV$*, *Phys. Rev. Lett.* **93** (2004) 072001 [hep-ex/0312021] [INSPIRE].

[14] D0 collaboration, *Observation and properties of the $X(3872)$ decaying to $J/\psi\pi^+\pi^-$ in $p\bar{p}$ collisions at $\sqrt{s} = 1.96\,TeV$*, *Phys. Rev. Lett.* **93** (2004) 162002 [hep-ex/0405004] [INSPIRE].

[15] BABAR collaboration, *Study of the $B^- \to J/\psi K^-\pi^+\pi^-$ decay and measurement of the $B^- \to X(3872)K^-$ branching fraction*, *Phys. Rev. D* **71** (2005) 071103 [hep-ex/0406022] [INSPIRE].

[16] CDF collaboration, *Measurement of the dipion mass spectrum in $X(3872) \to J/\psi\pi^+\pi^-$ decays.*, *Phys. Rev. Lett.* **96** (2006) 102002 [hep-ex/0512074] [INSPIRE].

[17] BABAR collaboration, *Study of the $X(3872)$ and $Y(4260)$ in $B^0 \to J/\psi\pi^+\pi^-K^0$ and $B^- \to J/\psi\pi^+\pi^-K^-$ decays*, *Phys. Rev. D* **73** (2006) 011101 [hep-ex/0507090] [INSPIRE].

[18] BABAR collaboration, *Search for $B^+ \to X(3872)K^+$, $X(3872) \to J/\psi\gamma$*, *Phys. Rev. D* **74** (2006) 071101 [hep-ex/0607050] [INSPIRE].

[19] CDF collaboration, *Analysis of the quantum numbers $J^{PC}$ of the $X(3872)$*, *Phys. Rev. Lett.* **98** (2007) 132002 [hep-ex/0612053] [INSPIRE].

[20] BABAR collaboration, *Search for prompt production of $\chi_c$ and $X(3872)$ in $e^+e^-$ annihilations*, *Phys. Rev. D* **76** (2007) 071102 [arXiv:0707.1633] [INSPIRE].

[21] BABAR collaboration, *Study of $B \to X(3872)K$, with $X(3872) \to J/\psi\pi^+\pi^-$*, *Phys. Rev. D* **77** (2008) 111101 [arXiv:0803.2838] [INSPIRE].

[22] CDF collaboration, *Precision measurement of the $X(3872)$ mass in $J/\psi\pi^+\pi^-$ decays*, *Phys. Rev. Lett.* **103** (2009) 152001 [arXiv:0906.5218] [INSPIRE].

[23] BABAR collaboration, *Evidence for $X(3872) \to \psi(2S)\gamma$ in $B^\pm \to X(3872)K^\pm$ decays, and a study of $B \to c\bar{c}\gamma K$*, *Phys. Rev. Lett.* **102** (2009) 132001 [arXiv:0809.0042] [INSPIRE].

[24] BELLE collaboration, *Study of the $B \to X(3872)(\to D^{*0}\bar{D}^0)K$ decay*, *Phys. Rev. D* **81** (2010) 031103 [arXiv:0810.0358] [INSPIRE].

[25] BaBar collaboration, *Evidence for the decay $X(3872) \to J/\psi\omega$*, *Phys. Rev. D* **82** (2010) 011101 [arXiv:1005.5190] [ɪɴSPIRE].

[26] Belle collaboration, *Bounds on the width, mass difference and other properties of $X(3872) \to \pi^+\pi^- J/\psi$ decays*, *Phys. Rev. D* **84** (2011) 052004 [arXiv:1107.0163] [ɪɴSPIRE].

[27] Belle collaboration, *Observation of $X(3872) \to J/\psi\gamma$ and search for $X(3872) \to \psi'\gamma$ in B decays*, *Phys. Rev. Lett.* **107** (2011) 091803 [arXiv:1105.0177] [ɪɴSPIRE].

[28] LHCb collaboration, *Observation of $X(3872)$ production in pp collisions at $\sqrt{s} = 7\,TeV$*, *Eur. Phys. J. C* **72** (2012) 1972 [arXiv:1112.5310] [ɪɴSPIRE].

[29] LHCb collaboration, *Determination of the $X(3872)$ meson quantum numbers*, *Phys. Rev. Lett.* **110** (2013) 222001 [arXiv:1302.6269] [ɪɴSPIRE].

[30] CMS collaboration, *Measurement of the $X(3872)$ production cross section via decays to $J/\psi\pi^+\pi^-$ in pp collisions at $\sqrt{s} = 7\,TeV$*, *JHEP* **04** (2013) 154 [arXiv:1302.3968] [ɪɴSPIRE].

[31] BESIII collaboration, *Observation of $e^+e^- \to \gamma X(3872)$ at BESIII*, *Phys. Rev. Lett.* **112** (2014) 092001 [arXiv:1310.4101] [ɪɴSPIRE].

[32] LHCb collaboration, *Evidence for the decay $X(3872) \to \psi(2S)\gamma$*, *Nucl. Phys. B* **886** (2014) 665 [arXiv:1404.0275] [ɪɴSPIRE].

[33] Belle collaboration, *Observation of $X(3872)$ in $B \to X(3872)K\pi$ decays*, *Phys. Rev. D* **91** (2015) 051101 [arXiv:1501.06867] [ɪɴSPIRE].

[34] LHCb collaboration, *Quantum numbers of the $X(3872)$ state and orbital angular momentum in its $\rho^0 J\psi$ decay*, *Phys. Rev. D* **92** (2015) 011102 [arXiv:1504.06339] [ɪɴSPIRE].

[35] ATLAS collaboration, *Measurements of $\psi(2S)$ and $X(3872) \to J/\psi\pi^+\pi^-$ production in pp collisions at $\sqrt{s} = 8\,TeV$ with the ATLAS detector*, *JHEP* **01** (2017) 117 [arXiv:1610.09303] [ɪɴSPIRE].

[36] LHCb collaboration, *Observation of $\eta_c(2S) \to p\bar{p}$ and search for $X(3872) \to p\bar{p}$ decays*, *Phys. Lett. B* **769** (2017) 305 [arXiv:1607.06446] [ɪɴSPIRE].

[37] LHCb collaboration, *Observation of the $\Lambda_b^0 \to \chi_{c1}(3872)pK^-$ decay*, *JHEP* **09** (2019) 028 [arXiv:1907.00954] [ɪɴSPIRE].

[38] Belle collaboration, *Search for $B^0 \to X(3872)\gamma$*, *Phys. Rev. D* **100** (2019) 012002 [arXiv:1905.11718] [ɪɴSPIRE].

[39] Belle collaboration, *Search for $X(3872)$ and $X(3915)$ decay into $\chi_{c1}\pi^0$ in B decays at Belle*, *Phys. Rev. D* **99** (2019) 111101 [arXiv:1904.07015] [ɪɴSPIRE].

[40] CMS collaboration, *Observation of the $B_s^0 \to X(3872)\phi$ decay*, arXiv:2005.04764 [ɪɴSPIRE].

[41] N.N. Achasov and E.V. Rogozina, *$X(3872), I^G(J^{PC}) = 0^+(1^{++})$, as the $\chi_{1c}(2P)$ charmonium*, *Mod. Phys. Lett. A* **30** (2015) 1550181 [arXiv:1501.03583] [ɪɴSPIRE].

[42] N.A. Törnqvist, *Isospin breaking of the narrow charmonium state of Belle at 3872 MeV as a deuson*, *Phys. Lett. B* **590** (2004) 209 [hep-ph/0402237] [ɪɴSPIRE].

[43] E.S. Swanson, *Short range structure in the $X(3872)$*, *Phys. Lett. B* **588** (2004) 189 [hep-ph/0311229] [ɪɴSPIRE].

[44] C.-Y. Wong, *Molecular states of heavy quark mesons*, *Phys. Rev. C* **69** (2004) 055202 [hep-ph/0311088] [INSPIRE].

[45] L. Maiani, F. Piccinini, A.D. Polosa and V. Riquer, *Diquark-antidiquarks with hidden or open charm and the nature of X(3872)*, *Phys. Rev. D* **71** (2005) 014028 [hep-ph/0412098] [INSPIRE].

[46] B.A. Li, *Is X(3872) a possible candidate of hybrid meson?*, *Phys. Lett. B* **605** (2005) 306 [hep-ph/0410264] [INSPIRE].

[47] K.K. Seth, *An alternative interpretation of X(3872)*, *Phys. Lett. B* **612** (2005) 1 [hep-ph/0411122] [INSPIRE].

[48] R.D. Matheus, F.S. Navarra, M. Nielsen and C.M. Zanetti, *QCD sum rules for the X(3872) as a mixed molecule-charmoniun state*, *Phys. Rev. D* **80** (2009) 056002 [arXiv:0907.2683] [INSPIRE].

[49] W. Chen, H.-y. Jin, R.T. Kleiv, T.G. Steele, M. Wang and Q. Xu, *QCD sum-rule interpretation of X(3872) with $J^{PC} = 1^{++}$ mixtures of hybrid charmonium and $\overline{D}D^*$ molecular currents*, *Phys. Rev. D* **88** (2013) 045027 [arXiv:1305.0244] [INSPIRE].

[50] E. Braaten, L.-P. He and K. Ingles, *Production of X(3872) accompanied by a pion in B meson decay*, *Phys. Rev. D* **100** (2019) 074028 [arXiv:1902.03259] [INSPIRE].

[51] LHCb collaboration, *Near-threshold $D\bar{D}$ spectroscopy and observation of a new charmonium state*, *JHEP* **07** (2019) 035 [arXiv:1903.12240] [INSPIRE].

[52] S. Piemonte, S. Collins, D. Mohler, M. Padmanath and S. Prelovsek, *Charmonium resonances with $J^{PC} = 1^{--}$ and $3^{--}$ from $\bar{D}D$ scattering on the lattice*, *Phys. Rev. D* **100** (2019) 074505 [arXiv:1905.03506] [INSPIRE].

[53] G.L. Yu and Z.G. Wang, *Analysis of the X(3842) as a D-wave charmonium meson*, *Int. J. Mod. Phys. A* **34** (2019) 1950151 [arXiv:1907.00341] [INSPIRE].

[54] E705 collaboration, *Search for hidden charm states decaying into $J/\psi$ or $\psi'$ plus pions*, *Phys. Rev. D* **50** (1994) 4258 [INSPIRE].

[55] BELLE collaboration, *Evidence of a new narrow resonance decaying to $\chi_{c1}\gamma$ in $B \to \chi_{c1}\gamma K$*, *Phys. Rev. Lett.* **111** (2013) 032001 [arXiv:1304.3975] [INSPIRE].

[56] BESIII collaboration, *Observation of the $\psi(1^3D_2)$ state in $e^+e^- \to \pi^+\pi^-\gamma\chi_{c1}$ at BESIII*, *Phys. Rev. Lett.* **115** (2015) 011803 [arXiv:1503.08203] [INSPIRE].

[57] D. Ebert, R.N. Faustov and V.O. Galkin, *Properties of heavy quarkonia and $B_c$ mesons in the relativistic quark model*, *Phys. Rev. D* **67** (2003) 014027 [hep-ph/0210381] [INSPIRE].

[58] E.J. Eichten, K. Lane and C. Quigg, *B-meson gateways to missing charmonium levels*, *Phys. Rev. Lett.* **89** (2002) 162002 [hep-ph/0206018] [INSPIRE].

[59] B. Wang, H. Xu, X. Liu, D.-Y. Chen, S. Coito and E. Eichten, *Using $X(3823) \to J/\psi\pi^+\pi^-$ to identify coupled-channel effects*, *Front. Phys.* **11** (2016) 111402 [arXiv:1507.07985] [INSPIRE].

[60] H. Xu, X. Liu and T. Matsuki, *Understanding $B^- \to X(3823)K^-$ via rescattering mechanism and predicting $B^- \to \eta_{c2}(^1D_2)/\psi_3(^3D_3)K^-$*, *Phys. Rev. D* **94** (2016) 034005 [arXiv:1605.04776] [INSPIRE].

[61] LHCb collaboration, *Study of the lineshape of the $\chi_{c1}(3872)$ state*, arXiv:2005.13419 [INSPIRE].

[62] LHCb collaboration, *The LHCb detector at the LHC*, 2008 *JINST* **3** S08005 [ɪɴSPIRE].

[63] LHCb collaboration, *LHCb detector performance*, *Int. J. Mod. Phys. A* **30** (2015) 1530022 [arXiv:1412.6352] [ɪɴSPIRE].

[64] R. Aaij et al., *Performance of the LHCb vertex locator*, 2014 *JINST* **9** P09007 [arXiv:1405.7808] [ɪɴSPIRE].

[65] LHCb OUTER TRACKER GROUP collaboration, *Performance of the LHCb Outer Tracker*, 2014 *JINST* **9** P01002 [arXiv:1311.3893] [ɪɴSPIRE].

[66] LHCb OUTER TRACKER GROUP collaboration, *Improved performance of the LHCb Outer Tracker in LHC Run 2*, 2017 *JINST* **12** P11016 [arXiv:1708.00819] [ɪɴSPIRE].

[67] LHCb collaboration, *Measurement of the $\Lambda_b^0$, $\Xi_b^-$ and $\Omega_b^-$ baryon masses*, *Phys. Rev. Lett.* **110** (2013) 182001 [arXiv:1302.1072] [ɪɴSPIRE].

[68] LHCb collaboration, *Precision measurement of D meson mass differences*, *JHEP* **06** (2013) 065 [arXiv:1304.6865] [ɪɴSPIRE].

[69] LHCb RICH GROUP collaboration, *Performance of the LHCb RICH detector at the LHC*, *Eur. Phys. J. C* **73** (2013) 2431 [arXiv:1211.6759] [ɪɴSPIRE].

[70] A.A. Alves Jr. et al., *Performance of the LHCb muon system*, 2013 *JINST* **8** P02022 [arXiv:1211.1346] [ɪɴSPIRE].

[71] R. Aaij et al., *The LHCb trigger and its performance in 2011*, 2013 *JINST* **8** P04022 [arXiv:1211.3055] [ɪɴSPIRE].

[72] T. Sjöstrand, S. Mrenna and P.Z. Skands, *A brief introduction to PYTHIA 8.1*, *Comput. Phys. Commun.* **178** (2008) 852 [arXiv:0710.3820] [ɪɴSPIRE].

[73] I. Belyaev et al., *Handling of the generation of primary events in Gauss, the LHCb simulation framework*, *J. Phys. Conf. Ser.* **331** (2011) 032047 [ɪɴSPIRE].

[74] D.J. Lange, *The EvtGen particle decay simulation package*, *Nucl. Instrum. Meth. A* **462** (2001) 152 [ɪɴSPIRE].

[75] P. Golonka and Z. Was, *PHOTOS Monte Carlo: a precision tool for QED corrections in Z and W decays*, *Eur. Phys. J. C* **45** (2006) 97 [hep-ph/0506026] [ɪɴSPIRE].

[76] K. Gottfried, *Hadronic transitions between quark-antiquark bound states*, *Phys. Rev. Lett.* **40** (1978) 598 [ɪɴSPIRE].

[77] M.B. Voloshin, *On dynamics of heavy quarks in nonperturbative QCD vacuum*, *Nucl. Phys. B* **154** (1979) 365 [ɪɴSPIRE].

[78] M.E. Peskin, *Short distance analysis for heavy quark systems. 1. Diagrammatics*, *Nucl. Phys. B* **156** (1979) 365 [ɪɴSPIRE].

[79] G. Bhanot and M.E. Peskin, *Short-distance analysis for heavy-quark systems. 2. Applications*, *Nucl. Phys. B* **156** (1979) 391 [ɪɴSPIRE].

[80] GEANT4 collaboration, *GEANT4 developments and applications*, *IEEE Trans. Nucl. Sci.* **53** (2006) 270.

[81] GEANT4 collaboration, *GEANT4 — a simulation toolkit*, *Nucl. Instrum. Meth. A* **506** (2003) 250 [ɪɴSPIRE].

[82] M. Clemencic et al., *The LHCb simulation application, Gauss: design, evolution and experience*, *J. Phys. Conf. Ser.* **331** (2011) 032023 [ɪɴSPIRE].

[83] LHCb collaboration, *Measurement of the track reconstruction efficiency at LHCb*, 2015 *JINST* **10** P02007 [`arXiv:1408.1251`] [INSPIRE].

[84] LHCb collaboration, *Measurement of relative branching fractions of B decays to $\psi(2S)$ and $J/\psi$ mesons*, *Eur. Phys. J. C* **72** (2012) 2118 [`arXiv:1205.0918`] [INSPIRE].

[85] LHCb collaboration, *Observation of $B_c^+ \to J/\psi D_s^+$ and $B_c^+ \to J/\psi D_s^{*+}$ decays*, *Phys. Rev. D* **87** (2013) 112012 [*Addendum ibid.* **89** (2014) 019901] [`arXiv:1304.4530`] [INSPIRE].

[86] LHCb collaboration, *Observation of $B_s^0 \to \chi_{c1}\phi$ decay and study of $B^0 \to \chi_{c1,2}K^{*0}$ decays*, *Nucl. Phys. B* **874** (2013) 663 [`arXiv:1305.6511`] [INSPIRE].

[87] LHCb collaboration, *Observation of the decay $B_c^+ \to J/\psi K^+ K^- \pi^+$*, *JHEP* **11** (2013) 094 [`arXiv:1309.0587`] [INSPIRE].

[88] LHCb collaboration, *Evidence for the decay $B_c^+ \to J/\psi 3\pi^+ 2\pi^-$*, *JHEP* **05** (2014) 148 [`arXiv:1404.0287`] [INSPIRE].

[89] LHCb collaboration, *Measurement of the lifetime of the $B_c^+$ meson using the $B_c^+ \to J/\psi \pi^+$ decay mode*, *Phys. Lett. B* **742** (2015) 29 [`arXiv:1411.6899`] [INSPIRE].

[90] LHCb collaboration, *Observation of $\Lambda_b^0 \to \psi(2S)pK^-$ and $\Lambda_b^0 \to J/\psi \pi^+ \pi^- pK^-$ decays and a measurement of the $\Lambda_b^0$ baryon mass*, *JHEP* **05** (2016) 132 [`arXiv:1603.06961`] [INSPIRE].

[91] LHCb collaboration, *Observation of $B^+ \to J/\psi 3\pi^+ 2\pi^-$ and $B^+ \to \psi(2S)\pi^+\pi^+\pi^-$ decays*, *Eur. Phys. J. C* **77** (2017) 72 [`arXiv:1610.01383`] [INSPIRE].

[92] LHCb collaboration, *Observation of the decay $\Lambda_b^0 \to \psi(2S)p\pi^-$*, *JHEP* **08** (2018) 131 [`arXiv:1806.08084`] [INSPIRE].

[93] LHCb collaboration, *Observation of new resonances in the $\Lambda_b^0 \pi^+ \pi^-$ system*, *Phys. Rev. Lett.* **123** (2019) 152001 [`arXiv:1907.13598`] [INSPIRE].

[94] LHCb collaboration, *Observation of a new baryon state in the $\Lambda_b^0 \pi^+ \pi^-$ mass spectrum*, *JHEP* **06** (2020) 136 [`arXiv:2002.05112`] [INSPIRE].

[95] L. Breiman, J.H. Friedman, R.A. Olshen and C.J. Stone, *Classification and regression trees*, Wadsworth international group, Belmont, California, U.S.A. (1984).

[96] A. Powell et al., *Particle identification at LHCb*, *PoS* **ICHEP2010** (2010) 020 [INSPIRE].

[97] W.D. Hulsbergen, *Decay chain fitting with a Kalman filter*, *Nucl. Instrum. Meth. A* **552** (2005) 566 [`physics/0503191`] [INSPIRE].

[98] S. Geisser, *Predictive inference: an introduction*, Chapman & Hall, New York, U.S.A. (1993).

[99] G. Punzi, *Sensitivity of searches for new signals and its optimization*, *eConf* **C 030908** (2003) MODT002 [`physics/0308063`] [INSPIRE].

[100] LHCb collaboration, *Observation of $J/\psi$-pair production in pp-collisions at $\sqrt{s} = 7\,TeV$*, *Phys. Lett. B* **707** (2012) 52 [`arXiv:1109.0963`] [INSPIRE].

[101] T. Skwarnicki, *A study of the radiative cascade transitions between the $\Upsilon'$ and $\Upsilon$ resonances*, Ph.D. thesis, Institute of Nuclear Physics, Krakow (1986), DESY-F31-86-02, INSPIRE.

[102] C. Hanhart, Yu.S. Kalashnikova, A.E. Kudryavtsev and A.V. Nefediev, *Reconciling the $X(3872)$ with the near-threshold enhancement in the $D^0 \bar{D}^{*0}$ final state*, *Phys. Rev. D* **76** (2007) 034007 [`arXiv:0704.0605`] [INSPIRE].

[103] E. Braaten and J. Stapleton, *Analysis of $J/\psi\pi^+\pi^-$ and $D^0\bar{D}^0\pi^0$ decays of the X(3872)*, *Phys. Rev. D* **81** (2010) 014019 [`arXiv:0907.3167`] [ɪɴSPIRE].

[104] Yu.S. Kalashnikova and A.V. Nefediev, *Nature of X(3872) from data*, *Phys. Rev. D* **80** (2009) 074004 [`arXiv:0907.4901`] [ɪɴSPIRE].

[105] P. Artoisenet, E. Braaten and D. Kang, *Using line shapes to discriminate between binding mechanisms for the X(3872)*, *Phys. Rev. D* **82** (2010) 014013 [`arXiv:1005.2167`] [ɪɴSPIRE].

[106] C. Hanhart, Yu.S. Kalashnikova and A.V. Nefediev, *Interplay of quark and meson degrees of freedom in a near-threshold resonance: multi-channel case*, *Eur. Phys. J. A* **47** (2011) 101 [`arXiv:1106.1185`] [ɪɴSPIRE].

[107] E. Byckling and K. Kajantie, *Particle kinematics*, John Wiley & Sons Inc., New York, U.S.A. (1973).

[108] S.S. Wilks, *The large-sample distribution of the likelihood ratio for testing composite hypotheses*, *Ann. Math. Stat.* **9** (1938) 60.

[109] R. Aaij et al., *Selection and processing of calibration samples to measure the particle identification performance of the LHCb experiment in Run 2*, *EPJ Tech. Instrum.* **6** (2019) 1 [`arXiv:1803.00824`] [ɪɴSPIRE].

[110] S. Jackman, *Bayesian analysis for the social sciences*, John Wiley & Sons, Inc., Hoboken, New Jersey, U.S.A. (2009).

[111] D. Martínez Santos and F. Dupertuis, *Mass distributions marginalized over per-event errors*, *Nucl. Instrum. Meth. A* **764** (2014) 150 [`arXiv:1312.5000`] [ɪɴSPIRE].

[112] BaBar collaboration, *Branching fraction measurements of the color-suppressed decays $\bar{B}^0 \to D^{(*)0}\pi^0$, $D^{(*)0}\eta$, $D^{(*)0}\omega$, and $D^{(*)0}\eta'$ and measurement of the polarization in the decay $\bar{B}^0 \to D^{*0}\omega$*, *Phys. Rev. D* **84** (2011) 112007 [*Erratum ibid.* **87** (2013) 039901] [`arXiv:1107.5751`] [ɪɴSPIRE].

[113] J.M. Blatt and V.F. Weisskopf, *Theoretical nuclear physics*, Springer, New York, U.S.A (1952), 10.1007/978-1-4612-9959-2 [ɪɴSPIRE].

[114] Y.-P. Kuang, S.F. Tuan and T.-M. Yan, *Hadronic transitions and $^1P_1$ states of heavy quarkonia*, *Phys. Rev. D* **37** (1988) 1210 [ɪɴSPIRE].

[115] X. Liu, X.-Q. Zeng and X.-Q. Li, *Study on contributions of hadronic loops to decays of $J/\psi \to vector + pseudoscalar mesons$*, *Phys. Rev. D* **74** (2006) 074003 [`hep-ph/0606191`] [ɪɴSPIRE].

[116] LHCb collaboration, *Measurements of $B_c^+$ production and mass with the $B_c^+ \to J/\psi\pi^+$ decay*, *Phys. Rev. Lett.* **109** (2012) 232001 [`arXiv:1209.5634`] [ɪɴSPIRE].

[117] LHCb collaboration, *Study of beauty hadron decays into pairs of charm hadrons*, *Phys. Rev. Lett.* **112** (2014) 202001 [`arXiv:1403.3606`] [ɪɴSPIRE].

[118] LHCb collaboration, *Precision measurement of the mass and lifetime of the $\Xi_b^0$ baryon*, *Phys. Rev. Lett.* **113** (2014) 032001 [`arXiv:1405.7223`] [ɪɴSPIRE].

[119] LHCb collaboration, *Precision measurement of the mass and lifetime of the $\Xi_b^-$ baryon*, *Phys. Rev. Lett.* **113** (2014) 242002 [`arXiv:1409.8568`] [ɪɴSPIRE].

[120] LHCb collaboration, *Measurement of the mass and lifetime of the $\Omega_b^-$ baryon*, *Phys. Rev. D* **93** (2016) 092007 [`arXiv:1604.01412`] [ɪɴSPIRE].

[121] LHCb collaboration, *Observation of the decays* $\Lambda_b^0 \to \chi_{c1} p K^-$ *and* $\Lambda_b^0 \to \chi_{c2} p K^-$, *Phys. Rev. Lett.* **119** (2017) 062001 [`arXiv:1704.07900`] [INSPIRE].

[122] LHCb collaboration, *Observation of an excited* $B_c^+$ *state*, *Phys. Rev. Lett.* **122** (2019) 232001 [`arXiv:1904.00081`] [INSPIRE].

[123] LHCb collaboration, *Precision measurement of the* $\Xi_{cc}^{++}$ *mass*, *JHEP* **02** (2020) 049 [`arXiv:1911.08594`] [INSPIRE].

[124] LHCb collaboration, *First observation of excited* $\Omega_b^-$ *states*, *Phys. Rev. Lett.* **124** (2020) 082002 [`arXiv:2001.00851`] [INSPIRE].

[125] LHCb collaboration, *Precision measurement of the* $B_c^+$ *meson mass*, *JHEP* **07** (2020) 123 [`arXiv:2004.08163`] [INSPIRE].

[126] M. Pivk and F.R. Le Diberder, *sPlot: a statistical tool to unfold data distributions*, *Nucl. Instrum. Meth. A* **555** (2005) 356 [`physics/0402083`] [INSPIRE].

# The LHCb collaboration

R. Aaij[31], C. Abellán Beteta[49], T. Ackernley[59], B. Adeva[45], M. Adinolfi[53], H. Afsharnia[9],
C.A. Aidala[82], S. Aiola[25], Z. Ajaltouni[9], S. Akar[64], J. Albrecht[14], F. Alessio[47], M. Alexander[58],
A. Alfonso Albero[44], Z. Aliouche[61], G. Alkhazov[37], P. Alvarez Cartelle[47], A.A. Alves Jr[45],
S. Amato[2], Y. Amhis[11], L. An[21], L. Anderlini[21], G. Andreassi[48], A. Andreianov[37],
M. Andreotti[20], F. Archilli[16], A. Artamonov[43], M. Artuso[67], K. Arzymatov[41], E. Aslanides[10],
M. Atzeni[49], B. Audurier[11], S. Bachmann[16], M. Bachmayer[48], J.J. Back[55], S. Baker[60],
P. Baladron Rodriguez[45], V. Balagura[11,b], W. Baldini[20], J. Baptista Leite[1], R.J. Barlow[61],
S. Barsuk[11], W. Barter[60], M. Bartolini[23,47,h], F. Baryshnikov[79], J.M. Basels[13], G. Bassi[28],
V. Batozskaya[35], B. Batsukh[67], A. Battig[14], A. Bay[48], M. Becker[14], F. Bedeschi[28], I. Bediaga[1],
A. Beiter[67], V. Belavin[41], S. Belin[26], V. Bellee[48], K. Belous[43], I. Belyaev[38], G. Bencivenni[22],
E. Ben-Haim[12], A. Berezhnoy[39], R. Bernet[49], D. Berninghoff[16], H.C. Bernstein[67], C. Bertella[47],
E. Bertholet[12], A. Bertolin[27], C. Betancourt[49], F. Betti[19,e], M.O. Bettler[54], Ia. Bezshyiko[49],
S. Bhasin[53], J. Bhom[33], L. Bian[72], M.S. Bieker[14], S. Bifani[52], P. Billoir[12], F.C.R. Bishop[54],
A. Bizzeti[21,t], M. Bjørn[62], M.P. Blago[47], T. Blake[55], F. Blanc[48], S. Blusk[67], D. Bobulska[58],
V. Bocci[30], J.A. Boelhauve[14], O. Boente Garcia[45], T. Boettcher[63], A. Boldyrev[80], A. Bondar[42,w],
N. Bondar[37,47], S. Borghi[61], M. Borisyak[41], M. Borsato[16], J.T. Borsuk[33], S.A. Bouchiba[48],
T.J.V. Bowcock[59], A. Boyer[47], C. Bozzi[20], M.J. Bradley[60], S. Braun[65], A. Brea Rodriguez[45],
M. Brodski[47], J. Brodzicka[33], A. Brossa Gonzalo[55], D. Brundu[26], E. Buchanan[53], A. Buonaura[49],
C. Burr[47], A. Bursche[26], A. Butkevich[40], J.S. Butter[31], J. Buytaert[47], W. Byczynski[47],
S. Cadeddu[26], H. Cai[72], R. Calabrese[20,g], L. Calero Diaz[22], S. Cali[22], R. Calladine[52], M. Calvi[24,i],
M. Calvo Gomez[44,l], P. Camargo Magalhaes[53], A. Camboni[44], P. Campana[22],
D.H. Campora Perez[31], A.F. Campoverde Quezada[5], S. Capelli[24,i], L. Capriotti[19,e],
A. Carbone[19,e], G. Carboni[29], R. Cardinale[23,h], A. Cardini[26], I. Carli[6], P. Carniti[24,i],
K. Carvalho Akiba[31], A. Casais Vidal[45], G. Casse[59], M. Cattaneo[47], G. Cavallero[47], S. Celani[48],
R. Cenci[28], J. Cerasoli[10], A.J. Chadwick[59], M.G. Chapman[53], M. Charles[12], Ph. Charpentier[47],
G. Chatzikonstantinidis[52], M. Chefdeville[8], C. Chen[3], S. Chen[26], A. Chernov[33], S.-G. Chitic[47],
V. Chobanova[45], S. Cholak[48], M. Chrzaszcz[33], A. Chubykin[37], V. Chulikov[37], P. Ciambrone[22],
M.F. Cicala[55], X. Cid Vidal[45], G. Ciezarek[47], F. Cindolo[19], P.E.L. Clarke[57], M. Clemencic[47],
H.V. Cliff[54], J. Closier[47], J.L. Cobbledick[61], V. Coco[47], J.A.B. Coelho[11], J. Cogan[10],
E. Cogneras[9], L. Cojocariu[36], P. Collins[47], T. Colombo[47], A. Contu[26], N. Cooke[52], G. Coombs[58],
S. Coquereau[44], G. Corti[47], C.M. Costa Sobral[55], B. Couturier[47], D.C. Craik[63], J. Crkovská[66],
M. Cruz Torres[1,y], R. Currie[57], C.L. Da Silva[66], E. Dall'Occo[14], J. Dalseno[45], C. D'Ambrosio[47],
A. Danilina[38], P. d'Argent[47], A. Davis[61], O. De Aguiar Francisco[47], K. De Bruyn[47],
S. De Capua[61], M. De Cian[48], J.M. De Miranda[1], L. De Paula[2], M. De Serio[18,d], D. De Simone[49],
P. De Simone[22], J.A. de Vries[77], C.T. Dean[66], W. Dean[82], D. Decamp[8], L. Del Buono[12],
B. Delaney[54], H.-P. Dembinski[14], A. Dendek[34], V. Denysenko[49], D. Derkach[80], O. Deschamps[9],
F. Desse[11], F. Dettori[26,f], B. Dey[7], A. Di Canto[47], P. Di Nezza[22], S. Didenko[79], H. Dijkstra[47],
V. Dobishuk[51], A.M. Donohoe[17], F. Dordei[26], A.C. dos Reis[1], L. Douglas[58],
A. Dovbnya[50], A.G. Downes[8], K. Dreimanis[59], M.W. Dudek[33], L. Dufour[47], P. Durante[47],
J.M. Durham[66], D. Dutta[61], M. Dziewiecki[16], A. Dziurda[33], A. Dzyuba[37], S. Easo[56], U. Egede[69],
V. Egorychev[38], S. Eidelman[42,w], S. Eisenhardt[57], S. Ek-In[48], L. Eklund[58], S. Ely[67], A. Ene[36],
E. Epple[66], S. Escher[13], J. Eschle[49], S. Esen[31], T. Evans[47], A. Falabella[19], J. Fan[3], Y. Fan[5],
B. Fang[72], N. Farley[52], S. Farry[59], D. Fazzini[11], P. Fedin[38], M. Féo[47], P. Fernandez Declara[47],
A. Fernandez Prieto[45], F. Ferrari[19,e], L. Ferreira Lopes[48], F. Ferreira Rodrigues[2],
S. Ferreres Sole[31], M. Ferrillo[49], M. Ferro-Luzzi[47], S. Filippov[40], R.A. Fini[18], M. Fiorini[20,g],
M. Firlej[34], K.M. Fischer[62], C. Fitzpatrick[61], T. Fiutowski[34], F. Fleuret[11,b], M. Fontana[47],

F. Fontanelli[23,h], R. Forty[47], V. Franco Lima[59], M. Franco Sevilla[65], M. Frank[47], E. Franzoso[20],
G. Frau[16], C. Frei[47], D.A. Friday[58], J. Fu[25,p], Q. Fuehring[14], W. Funk[47], E. Gabriel[57],
T. Gaintseva[41], A. Gallas Torreira[45], D. Galli[19,e], S. Gallorini[27], S. Gambetta[57], Y. Gan[3],
M. Gandelman[2], P. Gandini[25], Y. Gao[4], M. Garau[26], L.M. Garcia Martin[46], P. Garcia Moreno[44],
J. García Pardiñas[49], B. Garcia Plana[45], F.A. Garcia Rosales[11], L. Garrido[44], D. Gascon[44],
C. Gaspar[47], R.E. Geertsema[31], D. Gerick[16], E. Gersabeck[61], M. Gersabeck[61], T. Gershon[55],
D. Gerstel[10], Ph. Ghez[8], V. Gibson[54], A. Gioventù[45], P. Gironella Gironell[44], L. Giubega[36],
C. Giugliano[20,g], K. Gizdov[57], V.V. Gligorov[12], C. Göbel[70], E. Golobardes[44,l], D. Golubkov[38],
A. Golutvin[60,79], A. Gomes[1,a], M. Goncerz[33], P. Gorbounov[38], I.V. Gorelov[39], C. Gotti[24,i],
E. Govorkova[31], J.P. Grabowski[16], R. Graciani Diaz[44], T. Grammatico[12],
L.A. Granado Cardoso[47], E. Graugés[44], E. Graverini[48], G. Graziani[21], A. Grecu[36],
L.M. Greeven[31], P. Griffith[20,g], L. Grillo[61], L. Gruber[47], B.R. Gruberg Cazon[62], C. Gu[3],
M. Guarise[20], P. A. Günther[16], E. Gushchin[40], A. Guth[13], Yu. Guz[43,47], T. Gys[47],
T. Hadavizadeh[69], G. Haefeli[48], C. Haen[47], S.C. Haines[54], P.M. Hamilton[65], Q. Han[7], X. Han[16],
T.H. Hancock[62], S. Hansmann-Menzemer[16], N. Harnew[62], T. Harrison[59], R. Hart[31], C. Hasse[47],
M. Hatch[47], J. He[5], M. Hecker[60], K. Heijhoff[31], K. Heinicke[14], A.M. Hennequin[47], K. Hennessy[59],
L. Henry[25,46], J. Heuel[13], A. Hicheur[68], D. Hill[62], M. Hilton[61], S.E. Hollitt[14], P.H. Hopchev[48],
J. Hu[16], J. Hu[71], W. Hu[7], W. Huang[5], W. Hulsbergen[31], T. Humair[60], R.J. Hunter[55],
M. Hushchyn[80], D. Hutchcroft[59], D. Hynds[31], P. Ibis[14], M. Idzik[34], D. Ilin[37], P. Ilten[52],
A. Inglessi[37], K. Ivshin[37], R. Jacobsson[47], S. Jakobsen[47], E. Jans[31], B.K. Jashal[46], A. Jawahery[65],
V. Jevtic[14], F. Jiang[3], M. John[62], D. Johnson[47], C.R. Jones[54], T.P. Jones[55], B. Jost[47], N. Jurik[62],
S. Kandybei[50], Y. Kang[3], M. Karacson[47], J.M. Kariuki[53], N. Kazeev[80], M. Kecke[16],
F. Keizer[54,47], M. Kelsey[67], M. Kenzie[55], T. Ketel[32], B. Khanji[47], A. Kharisova[81], K.E. Kim[67],
T. Kirn[13], V.S. Kirsebom[48], O. Kitouni[63], S. Klaver[22], K. Klimaszewski[35], S. Koliiev[51],
A. Kondybayeva[79], A. Konoplyannikov[38], P. Kopciewicz[34], R. Kopecna[16], P. Koppenburg[31],
M. Korolev[39], I. Kostiuk[31,51], O. Kot[51], S. Kotriakhova[37], P. Kravchenko[37], L. Kravchuk[40],
R.D. Krawczyk[47], M. Kreps[55], F. Kress[60], S. Kretzschmar[13], P. Krokovny[42,w], W. Krupa[34],
W. Krzemien[35], W. Kucewicz[33,k], M. Kucharczyk[33], V. Kudryavtsev[42,w], H.S. Kuindersma[31],
G.J. Kunde[66], T. Kvaratskheliya[38], D. Lacarrere[47], G. Lafferty[61], A. Lai[26], A. Lampis[26],
D. Lancierini[49], J.J. Lane[61], R. Lane[53], G. Lanfranchi[22], C. Langenbruch[13], O. Lantwin[49,79],
T. Latham[55], F. Lazzari[28,u], R. Le Gac[10], S.H. Lee[82], R. Lefèvre[9], A. Leflat[39,47], O. Leroy[10],
T. Lesiak[33], B. Leverington[16], H. Li[71], L. Li[62], X. Li[66], Y. Li[6], Y. Li[6], Z. Li[67], X. Liang[67],
T. Lin[60], R. Lindner[47], V. Lisovskyi[14], R. Litvinov[26], G. Liu[71], H. Liu[5], S. Liu[6], X. Liu[3],
A. Loi[26], J. Lomba Castro[45], I. Longstaff[58], J.H. Lopes[2], G. Loustau[49], G.H. Lovell[54], Y. Lu[6],
D. Lucchesi[27,n], S. Luchuk[40], M. Lucio Martinez[31], V. Lukashenko[31], Y. Luo[3], A. Lupato[61],
E. Luppi[20,g], O. Lupton[55], A. Lusiani[28,s], X. Lyu[5], L. Ma[6], S. Maccolini[19,e], F. Machefert[11],
F. Maciuc[36], V. Macko[48], P. Mackowiak[14], S. Maddrell-Mander[53], L.R. Madhan Mohan[53],
O. Maev[37], A. Maevskiy[80], D. Maisuzenko[37], M.W. Majewski[34], S. Malde[62], B. Malecki[47],
A. Malinin[78], T. Maltsev[42,w], H. Malygina[16], G. Manca[26,f], G. Mancinelli[10],
R. Manera Escalero[44], D. Manuzzi[19,e], D. Marangotto[25,p], J. Maratas[9,v], J.F. Marchand[8],
U. Marconi[19], S. Mariani[21,47,21], C. Marin Benito[11], M. Marinangeli[48], P. Marino[48], J. Marks[16],
P.J. Marshall[59], G. Martellotti[30], L. Martinazzoli[47], M. Martinelli[24,i], D. Martinez Santos[45],
F. Martinez Vidal[46], A. Massafferri[1], M. Materok[13], R. Matev[47], A. Mathad[49], Z. Mathe[47],
V. Matiunin[38], C. Matteuzzi[24], K.R. Mattioli[82], A. Mauri[49], E. Maurice[11,b], M. Mazurek[35],
M. McCann[60], L. Mcconnell[17], T.H. Mcgrath[61], A. McNab[61], R. McNulty[17], J.V. Mead[59],
B. Meadows[64], C. Meaux[10], G. Meier[14], N. Meinert[75], D. Melnychuk[35], S. Meloni[24,i], M. Merk[31],
A. Merli[25], L. Meyer Garcia[2], M. Mikhasenko[47], D.A. Milanes[73], E. Millard[55], M.-N. Minard[8],
O. Mineev[38], L. Minzoni[20,g], S.E. Mitchell[57], B. Mitreska[61], D.S. Mitzel[47], A. Mödden[14],

R.A. Mohammed[62], R.D. Moise[60], T. Mombächer[14], I.A. Monroy[73], S. Monteil[9], M. Morandin[27],
G. Morello[22], M.J. Morello[28,s], J. Moron[34], A.B. Morris[10], A.G. Morris[55], R. Mountain[67],
H. Mu[3], F. Muheim[57], M. Mukherjee[7], M. Mulder[47], D. Müller[47], K. Müller[49], C.H. Murphy[62],
D. Murray[61], P. Muzzetto[26], P. Naik[53], T. Nakada[48], R. Nandakumar[56], T. Nanut[48], I. Nasteva[2],
M. Needham[57], I. Neri[20,g], N. Neri[25,p], S. Neubert[74], N. Neufeld[47], R. Newcombe[60],
T.D. Nguyen[48], C. Nguyen-Mau[48,m], E.M. Niel[11], S. Nieswand[13], N. Nikitin[39], N.S. Nolte[47],
C. Nunez[82], A. Oblakowska-Mucha[34], V. Obraztsov[43], S. Ogilvy[58], D.P. O'Hanlon[53],
R. Oldeman[26,f], C.J.G. Onderwater[76], J. D. Osborn[82], A. Ossowska[33], J.M. Otalora Goicochea[2],
T. Ovsiannikova[38], P. Owen[49], A. Oyanguren[46], B. Pagare[55], P.R. Pais[47], T. Pajero[28,28,47,s],
A. Palano[18], M. Palutan[22], Y. Pan[61], G. Panshin[81], A. Papanestis[56], M. Pappagallo[57],
L.L. Pappalardo[20,g], C. Pappenheimer[64], W. Parker[65], C. Parkes[61], C.J. Parkinson[45],
G. Passaleva[21,47], A. Pastore[18], M. Patel[60], C. Patrignani[19,e], A. Pearce[47], A. Pellegrino[31],
M. Pepe Altarelli[47], S. Perazzini[19], D. Pereima[38], P. Perret[9], K. Petridis[53], A. Petrolini[23,h],
A. Petrov[78], S. Petrucci[57], M. Petruzzo[25], A. Philippov[41], L. Pica[28], B. Pietrzyk[8], G. Pietrzyk[48],
M. Pili[62], D. Pinci[30], J. Pinzino[47], F. Pisani[47], A. Piucci[16], V. Placinta[36], S. Playfer[57], J. Plews[52],
M. Plo Casasus[45], F. Polci[12], M. Poli Lener[22], M. Poliakova[67], A. Poluektov[10], N. Polukhina[79,c],
I. Polyakov[67], E. Polycarpo[2], G.J. Pomery[53], S. Ponce[47], A. Popov[43], D. Popov[5,47], S. Popov[41],
S. Poslavskii[43], K. Prasanth[33], L. Promberger[47], C. Prouve[45], V. Pugatch[51], A. Puig Navarro[49],
H. Pullen[62], G. Punzi[28,o], W. Qian[5], J. Qin[5], R. Quagliani[12], B. Quintana[8], N.V. Raab[17],
R.I. Rabadan Trejo[10], B. Rachwal[34], J.H. Rademacker[53], M. Rama[28], M. Ramos Pernas[45],
M.S. Rangel[2], F. Ratnikov[41,80], G. Raven[32], M. Reboud[8], F. Redi[48], F. Reiss[12],
C. Remon Alepuz[46], Z. Ren[3], V. Renaudin[62], R. Ribatti[28], S. Ricciardi[56], D.S. Richards[56],
K. Rinnert[59], P. Robbe[11], A. Robert[12], G. Robertson[57], A.B. Rodrigues[48], E. Rodrigues[59],
J.A. Rodriguez Lopez[73], M. Roehrken[47], A. Rollings[62], V. Romanovskiy[43], M. Romero Lamas[45],
A. Romero Vidal[45], J.D. Roth[82], M. Rotondo[22], M.S. Rudolph[67], T. Ruf[47], J. Ruiz Vidal[46],
A. Ryzhikov[80], J. Ryzka[34], J.J. Saborido Silva[45], N. Sagidova[37], N. Sahoo[55], B. Saitta[26,f],
C. Sanchez Gras[31], C. Sanchez Mayordomo[46], R. Santacesaria[30], C. Santamarina Rios[45],
M. Santimaria[22], E. Santovetti[29,j], G. Sarpis[61], M. Sarpis[74], A. Sarti[30], C. Satriano[30,r],
A. Satta[29], M. Saur[5], D. Savrina[38,39], H. Sazak[9], L.G. Scantlebury Smead[62], S. Schael[13],
M. Schellenberg[14], M. Schiller[58], H. Schindler[47], M. Schmelling[15], T. Schmelzer[14], B. Schmidt[47],
O. Schneider[48], A. Schopper[47], H.F. Schreiner[64], M. Schubiger[31], S. Schulte[48], M.H. Schune[11],
R. Schwemmer[47], B. Sciascia[22], A. Sciubba[22], S. Sellam[68], A. Semennikov[38], A. Sergi[52,47],
N. Serra[49], J. Serrano[10], L. Sestini[27], A. Seuthe[14], P. Seyfert[47], D.M. Shangase[82], M. Shapkin[43],
L. Shchutska[48], T. Shears[59], L. Shekhtman[42,w], V. Shevchenko[78], E.B. Shields[24,i], E. Shmanin[79],
J.D. Shupperd[67], B.G. Siddi[20], R. Silva Coutinho[49], L. Silva de Oliveira[2], G. Simi[27,n],
S. Simone[18,d], I. Skiba[20,g], N. Skidmore[74], T. Skwarnicki[67], M.W. Slater[52], J.C. Smallwood[62],
J.G. Smeaton[54], A. Smetkina[38], E. Smith[13], M. Smith[60], A. Snoch[31], M. Soares[19],
L. Soares Lavra[9], M.D. Sokoloff[64], F.J.P. Soler[58], A. Solovev[37], I. Solovyev[37],
F.L. Souza De Almeida[2], B. Souza De Paula[2], B. Spaan[14], E. Spadaro Norella[25,p], P. Spradlin[58],
F. Stagni[47], M. Stahl[64], S. Stahl[47], P. Stefko[48], O. Steinkamp[49,79], S. Stemmle[16], O. Stenyakin[43],
H. Stevens[14], S. Stone[67], S. Stracka[28], M.E. Stramaglia[48], M. Straticiuc[36], D. Strekalina[79],
S. Strokov[81], F. Suljik[62], J. Sun[26], L. Sun[72], Y. Sun[65], P. Svihra[61], P.N. Swallow[52],
K. Swientek[34], A. Szabelski[35], T. Szumlak[34], M. Szymanski[47], S. Taneja[61], Z. Tang[3],
T. Tekampe[14], F. Teubert[47], E. Thomas[47], K.A. Thomson[59], M.J. Tilley[60], V. Tisserand[9],
S. T'Jampens[8], M. Tobin[6], S. Tolk[47], L. Tomassetti[20,g], D. Torres Machado[1], D.Y. Tou[12],
M. Traill[58], M.T. Tran[48], E. Trifonova[79], C. Trippl[48], A. Tsaregorodtsev[10], G. Tuci[28,o],
A. Tully[48], N. Tuning[31], A. Ukleja[35], D.J. Unverzagt[16], A. Usachov[31], A. Ustyuzhanin[41,80],
U. Uwer[16], A. Vagner[81], V. Vagnoni[19], A. Valassi[47], G. Valenti[19], M. van Beuzekom[31],

H. Van Hecke[66], E. van Herwijnen[79], C.B. Van Hulse[17], M. van Veghel[76], R. Vazquez Gomez[45],
P. Vazquez Regueiro[45], C. Vázquez Sierra[31], S. Vecchi[20], J.J. Velthuis[53], M. Veltri[21,q],
A. Venkateswaran[67], M. Veronesi[31], M. Vesterinen[55], D. Vieira[64], M. Vieites Diaz[48],
H. Viemann[75], X. Vilasis-Cardona[83,44,l], E. Vilella Figueras[59], P. Vincent[12], G. Vitali[28],
A. Vitkovskiy[31], A. Vollhardt[49], D. Vom Bruch[12], A. Vorobyev[37], V. Vorobyev[42,w],
N. Voropaev[37], R. Waldi[75], J. Walsh[28], J. Wang[3], J. Wang[72], J. Wang[4], J. Wang[6], M. Wang[3],
R. Wang[53], Y. Wang[7], Z. Wang[49], D.R. Ward[54], H.M. Wark[59], N.K. Watson[52], S.G. Weber[12],
D. Websdale[60], C. Weisser[63], B.D.C. Westhenry[53], D.J. White[61], M. Whitehead[53], D. Wiedner[14],
G. Wilkinson[62], M. Wilkinson[67], I. Williams[54], M. Williams[63,69], M.R.J. Williams[61],
F.F. Wilson[56], W. Wislicki[35], M. Witek[33], L. Witola[16], G. Wormser[11], S.A. Wotton[54], H. Wu[67],
K. Wyllie[47], Z. Xiang[5], D. Xiao[7], Y. Xie[7], H. Xing[71], A. Xu[4], J. Xu[5], L. Xu[3], M. Xu[7], Q. Xu[5],
Z. Xu[4], D. Yang[3], Y. Yang[5], Z. Yang[3], Z. Yang[65], Y. Yao[67], L.E. Yeomans[59], H. Yin[7], J. Yu[7],
X. Yuan[67], O. Yushchenko[43], K.A. Zarebski[52], M. Zavertyaev[15,c], M. Zdybal[33], O. Zenaiev[47],
M. Zeng[3], D. Zhang[7], L. Zhang[3], S. Zhang[4], Y. Zhang[47], A. Zhelezov[16], Y. Zheng[5], X. Zhou[5],
Y. Zhou[5], X. Zhu[3], V. Zhukov[13,39], J.B. Zonneveld[57], S. Zucchelli[19,e], D. Zuliani[27], G. Zunica[61].

1    Centro Brasileiro de Pesquisas Físicas (CBPF), Rio de Janeiro, Brazil
2    Universidade Federal do Rio de Janeiro (UFRJ), Rio de Janeiro, Brazil
3    Center for High Energy Physics, Tsinghua University, Beijing, China
4    School of Physics State Key Laboratory of Nuclear Physics and Technology, Peking University,
     Beijing, China
5    University of Chinese Academy of Sciences, Beijing, China
6    Institute Of High Energy Physics (IHEP), Beijing, China
7    Institute of Particle Physics, Central China Normal University, Wuhan, Hubei, China
8    Univ. Grenoble Alpes, Univ. Savoie Mont Blanc, CNRS, IN2P3-LAPP, Annecy, France
9    Université Clermont Auvergne, CNRS/IN2P3, LPC, Clermont-Ferrand, France
10   Aix Marseille Univ, CNRS/IN2P3, CPPM, Marseille, France
11   Université Paris-Saclay, CNRS/IN2P3, IJCLab, Orsay, France
12   LPNHE, Sorbonne Université, Paris Diderot Sorbonne Paris Cité, CNRS/IN2P3, Paris, France
13   I. Physikalisches Institut, RWTH Aachen University, Aachen, Germany
14   Fakultät Physik, Technische Universität Dortmund, Dortmund, Germany
15   Max-Planck-Institut für Kernphysik (MPIK), Heidelberg, Germany
16   Physikalisches Institut, Ruprecht-Karls-Universität Heidelberg, Heidelberg, Germany
17   School of Physics, University College Dublin, Dublin, Ireland
18   INFN Sezione di Bari, Bari, Italy
19   INFN Sezione di Bologna, Bologna, Italy
20   INFN Sezione di Ferrara, Ferrara, Italy
21   INFN Sezione di Firenze, Firenze, Italy
22   INFN Laboratori Nazionali di Frascati, Frascati, Italy
23   INFN Sezione di Genova, Genova, Italy
24   INFN Sezione di Milano-Bicocca, Milano, Italy
25   INFN Sezione di Milano, Milano, Italy
26   INFN Sezione di Cagliari, Monserrato, Italy
27   INFN Sezione di Padova, Padova, Italy
28   INFN Sezione di Pisa, Pisa, Italy
29   INFN Sezione di Roma Tor Vergata, Roma, Italy
30   INFN Sezione di Roma La Sapienza, Roma, Italy
31   Nikhef National Institute for Subatomic Physics, Amsterdam, Netherlands
32   Nikhef National Institute for Subatomic Physics and VU University Amsterdam, Amsterdam,
     Netherlands
33   Henryk Niewodniczanski Institute of Nuclear Physics Polish Academy of Sciences, Kraków, Poland

34  *AGH - University of Science and Technology, Faculty of Physics and Applied Computer Science, Kraków, Poland*

35  *National Center for Nuclear Research (NCBJ), Warsaw, Poland*

36  *Horia Hulubei National Institute of Physics and Nuclear Engineering, Bucharest-Magurele, Romania*

37  *Petersburg Nuclear Physics Institute NRC Kurchatov Institute (PNPI NRC KI), Gatchina, Russia*

38  *Institute of Theoretical and Experimental Physics NRC Kurchatov Institute (ITEP NRC KI), Moscow, Russia, Moscow, Russia*

39  *Institute of Nuclear Physics, Moscow State University (SINP MSU), Moscow, Russia*

40  *Institute for Nuclear Research of the Russian Academy of Sciences (INR RAS), Moscow, Russia*

41  *Yandex School of Data Analysis, Moscow, Russia*

42  *Budker Institute of Nuclear Physics (SB RAS), Novosibirsk, Russia*

43  *Institute for High Energy Physics NRC Kurchatov Institute (IHEP NRC KI), Protvino, Russia, Protvino, Russia*

44  *ICCUB, Universitat de Barcelona, Barcelona, Spain*

45  *Instituto Galego de Física de Altas Enerxías (IGFAE), Universidade de Santiago de Compostela, Santiago de Compostela, Spain*

46  *Instituto de Fisica Corpuscular, Centro Mixto Universidad de Valencia - CSIC, Valencia, Spain*

47  *European Organization for Nuclear Research (CERN), Geneva, Switzerland*

48  *Institute of Physics, Ecole Polytechnique Fédérale de Lausanne (EPFL), Lausanne, Switzerland*

49  *Physik-Institut, Universität Zürich, Zürich, Switzerland*

50  *NSC Kharkiv Institute of Physics and Technology (NSC KIPT), Kharkiv, Ukraine*

51  *Institute for Nuclear Research of the National Academy of Sciences (KINR), Kyiv, Ukraine*

52  *University of Birmingham, Birmingham, United Kingdom*

53  *H.H. Wills Physics Laboratory, University of Bristol, Bristol, United Kingdom*

54  *Cavendish Laboratory, University of Cambridge, Cambridge, United Kingdom*

55  *Department of Physics, University of Warwick, Coventry, United Kingdom*

56  *STFC Rutherford Appleton Laboratory, Didcot, United Kingdom*

57  *School of Physics and Astronomy, University of Edinburgh, Edinburgh, United Kingdom*

58  *School of Physics and Astronomy, University of Glasgow, Glasgow, United Kingdom*

59  *Oliver Lodge Laboratory, University of Liverpool, Liverpool, United Kingdom*

60  *Imperial College London, London, United Kingdom*

61  *Department of Physics and Astronomy, University of Manchester, Manchester, United Kingdom*

62  *Department of Physics, University of Oxford, Oxford, United Kingdom*

63  *Massachusetts Institute of Technology, Cambridge, MA, United States*

64  *University of Cincinnati, Cincinnati, OH, United States*

65  *University of Maryland, College Park, MD, United States*

66  *Los Alamos National Laboratory (LANL), Los Alamos, United States*

67  *Syracuse University, Syracuse, NY, United States*

68  *Laboratory of Mathematical and Subatomic Physics , Constantine, Algeria, associated to [2]*

69  *School of Physics and Astronomy, Monash University, Melbourne, Australia, associated to [55]*

70  *Pontifícia Universidade Católica do Rio de Janeiro (PUC-Rio), Rio de Janeiro, Brazil, associated to [2]*

71  *Guangdong Provencial Key Laboratory of Nuclear Science, Institute of Quantum Matter, South China Normal University, Guangzhou, China, associated to [3]*

72  *School of Physics and Technology, Wuhan University, Wuhan, China, associated to [3]*

73  *Departamento de Fisica , Universidad Nacional de Colombia, Bogota, Colombia, associated to [12]*

74  *Universität Bonn - Helmholtz-Institut für Strahlen und Kernphysik, Bonn, Germany, associated to [16]*

75  *Institut für Physik, Universität Rostock, Rostock, Germany, associated to [16]*

76  *Van Swinderen Institute, University of Groningen, Groningen, Netherlands, associated to [31]*

77  *Universiteit Maastricht, Maastricht, Netherlands, associated to [31]*

[78] National Research Centre Kurchatov Institute, Moscow, Russia, associated to [38]

[79] National University of Science and Technology "MISIS", Moscow, Russia, associated to [38]

[80] National Research University Higher School of Economics, Moscow, Russia, associated to [41]

[81] National Research Tomsk Polytechnic University, Tomsk, Russia, associated to [38]

[82] University of Michigan, Ann Arbor, United States, associated to [67]

[83] DS4DS, La Salle, Universitat Ramon Llull, Barcelona, Spain


[a] Universidade Federal do Triângulo Mineiro (UFTM), Uberaba-MG, Brazil

[b] Laboratoire Leprince-Ringuet, Palaiseau, France

[c] P.N. Lebedev Physical Institute, Russian Academy of Science (LPI RAS), Moscow, Russia

[d] Università di Bari, Bari, Italy

[e] Università di Bologna, Bologna, Italy

[f] Università di Cagliari, Cagliari, Italy

[g] Università di Ferrara, Ferrara, Italy

[h] Università di Genova, Genova, Italy

[i] Università di Milano Bicocca, Milano, Italy

[j] Università di Roma Tor Vergata, Roma, Italy

[k] AGH - University of Science and Technology, Faculty of Computer Science, Electronics and Telecommunications, Kraków, Poland

[l] DS4DS, La Salle, Universitat Ramon Llull, Barcelona, Spain

[m] Hanoi University of Science, Hanoi, Vietnam

[n] Università di Padova, Padova, Italy

[o] Università di Pisa, Pisa, Italy

[p] Università degli Studi di Milano, Milano, Italy

[q] Università di Urbino, Urbino, Italy

[r] Università della Basilicata, Potenza, Italy

[s] Scuola Normale Superiore, Pisa, Italy

[t] Università di Modena e Reggio Emilia, Modena, Italy

[u] Università di Siena, Siena, Italy

[v] MSU - Iligan Institute of Technology (MSU-IIT), Iligan, Philippines

[w] Novosibirsk State University, Novosibirsk, Russia

[x] INFN Sezione di Trieste, Trieste, Italy

[y] Universidad Nacional Autonoma de Honduras, Tegucigalpa, Honduras